Nanoscale

ROYAL SOCIETY
OF **CHEMISTRY**

REVIEW ARTICLE
Yuichi Negishi *et al.*
Atomic-level separation of thiolate-protected metal clusters

NCNST

REVIEW

Atomic-level separation of thiolate-protected metal clusters

Yuichi Negishi, [iD] *[a,b] Sayaka Hashimoto,[a] Ayano Ebina,[a] Kota Hamada,[a]
Sakiat Hossain [iD] [a] and Tokuhisa Kawawaki [iD] [a,b]

Fine metal clusters have attracted much attention from the viewpoints of both basic and applied science for many years because of their unique physical/chemical properties and functions, which differ from those of bulk metals. Among these materials, thiolate (SR)-protected gold clusters ($Au_n(SR)_m$ clusters) have been the most studied metal clusters since 2000 because of their ease of synthesis and handling. However, in the early 2000s, it was not easy to isolate these metal clusters. Therefore, high-resolution separation methods were explored, and several atomic-level separation methods, including polyacryl-amide gel electrophoresis (PAGE), high-performance liquid chromatography (HPLC), and thin-layer chromatography (TLC), were successively established. These techniques have made it possible to isolate a series of $Au_n(SR)_m$ clusters, and much knowledge has been obtained on the correlation between the chemical composition and fundamental properties such as the stability, electronic structure, and physical properties of $Au_n(SR)_m$ clusters. In addition, these high-resolution separation techniques are now also fre-quently used to evaluate the distribution of the product and to track the reaction process. In this way, high-resolution separation techniques have played an essential role in the study of $Au_n(SR)_m$ clusters. However, only a few reviews have focused on this work. This review focuses on PAGE, HPLC, and TLC separation techniques, which offer high resolution and repeatability, and summarizes previous studies on the high-resolution separation of $Au_n(SR)_m$ and related clusters with the purpose of promoting a better understanding of the features and the utility of these techniques.

[a]*Department of Applied Chemistry, Faculty of Science, Tokyo University of Science, 1-3 Kagurazaka, Shinjuku-ku, Tokyo 162-8601, Japan. E-mail: negishi@rs.tus.ac.jp; Fax: +81-3-5261-4631; Tel: +81-3-5228-9145*
[b]*Research Institute for Science & Technology, Tokyo University of Science, 1-3 Kagurazaka, Shinjuku-ku, Tokyo 162-8601, Japan*

1. Introduction

Fine metal clusters smaller than ~2 nm ($\lesssim$100 atoms) exhibit different geometrical/electronic structures than those of bulk

Yuichi Negishi: Professor at the Department of Applied Chemistry at Tokyo University of Science. He received his Ph.D. degree in chemistry in 2001 under the supervision of Prof. Atsushi Nakajima from Keio University. Before joining Tokyo University of Science in 2008, he was employed as an assistant professor at Keio University and at the Institute for Molecular Science. His current research interests include the precise syn-thesis of stable and functionalized metal nanoclusters and their applications in energy and environmental materials.

Yuichi Negishi

Sayaka Hashimoto: Master course student in the Negishi group at Tokyo University of Science. She received her B.Sc. (2018) in chemistry from Tokyo University of Science. Her research interests include the development of precise synthesis methods for new noble metal nanoclusters based on high-per-formance liquid chromato-graphy.

Sayaka Hashimoto

metals.[1] Metal clusters often form a unique framework, such as an icosahedral structure, to suppress the surface energy instead of the close-packed structure often observed in bulk metals. In addition, metal clusters exhibit a discrete electronic structure unlike bulk metals. Because of these characteristic geometrical/electronic structures, fine metal clusters exhibit unique physical/chemical properties and functions that differ from those of bulk metals. In addition, the physical/chemical properties and functions of metal clusters vary significantly depending on the number of constituent atoms. For these reasons, fine metal clusters have attracted considerable attention for many years in the fields of both basic and applied science.

For these metal clusters, it is essential to conduct investigations on metal clusters controlled with atomic precision to understand the structures and physical/chemical properties. For this purpose, gas-phase beam experiments are superior[2–6] and they led the research studies on metal clusters in the 1980s and the 1990s. Many unique characteristics of metal clusters were discovered during this period by observing the mass distributions and electronic structures in gas-phase beam experiments. In parallel with such physical experiments, the research on the synthesis of phosphine (PR_3)-protected metal clusters was also actively pursued during this period.[7–15] The main purpose of these studies was to reveal the correlation between the chemical composition and geometrical structure, and the geometrical structures of some PR_3-protected metal clusters were determined by single-crystal X-ray diffraction (SC-XRD) at that time. Regarding the thiolate (SR)-protected metal clusters described below, the geometrical structure was first determined by SC-XRD in 2007; thus, the development of the research studies on PR_3-protected metal clusters at that time was remarkable. Since 2000, nanotechnology has been adopted as a national policy in many countries, and the main target metal clusters have shifted to SR-protected gold clusters ($Au_n(SR)_m$ clusters).[16–33] $Au_n(SR)_m$ clusters can be synthesized by simply mixing reagents in a solvent in air. Furthermore, $Au_n(SR)_m$ clusters are stable both in solution and in the solid state because the SR group forms a strong bond with Au. Such $Au_n(SR)_m$ clusters have a low threshold even for researchers

who have not worked on metal cluster synthesis and show great potential for material applications. It is presumed that these factors are largely related to the explosive increase in the number of studies on $Au_n(SR)_m$ clusters since 2000.[20]

However, for $Au_n(SR)_m$ clusters, single crystallization techniques could not be found, and thus, they could not be isolated in the early stage. Then, high-resolution separation techniques were developed to isolate $Au_n(SR)_m$ clusters. In earlier studies, separation techniques that relied on the differences in the solubility of solvents were mainly used.[34–38] Then, atomic-level separation techniques, such as polyacrylamide gel electrophoresis (PAGE) and liquid chromatography (LC) were developed. These methods made it possible to isolate a series of $Au_n(SR)_m$ clusters and obtain knowledge on the correlation between the chemical composition and the fundamental properties (e.g., stability,[39,40] electronic structure,[41] and physical/chemical properties[42,43]) of $Au_n(SR)_m$ clusters. After these separation techniques were established, the experimental conditions for synthesizing only stable metal clusters were also determined by using the features of their optical absorption spectra. As a result, several methods were established for selectively synthesizing stable $Au_n(SR)_m$ clusters with atomic precision.[24,44] In addition, because crystallization was easier for isolated or selectively synthesized $Au_n(SR)_m$ clusters, the geometrical structures were also determined by SC-XRD for several $Au_n(SR)_m$ clusters.[45] In parallel with these studies, studies on the application of these precisely controlled $Au_n(SR)_m$ and related clusters for chemical sensors,[46,47] photosensitization,[48] catalysts,[49,50] and solar cells[51,52] were conducted.[53]

Thus, high-resolution separation techniques have played an extremely important role in the study of $Au_n(SR)_m$ clusters. Recently, some stable metal clusters can be synthesized with atomic precision.[24,44] However, not all clusters can currently be synthesized size-selectively. Thus, the use of high-resolution separation techniques remains indispensable for understanding the correlation between the chemical composition and structure/physical properties of SR-protected metal clusters. Moreover, these separation techniques are also needed for purification of the main products and for isolation of metastable species. In addition to the use for fractionation as

Ayano Ebina: Master course student in the Negishi group at Tokyo University of Science. She received her B.Sc. (2019) in chemistry from Tokyo University of Science. Her research interests include the development of new high-resolution separation methods for noble metal nanoclusters.

Ayano Ebina

Kota Hamada: Master course student in the Negishi group at Tokyo University of Science. He received his B.Sc. (2018) in chemistry from Tokyo University of Science. In 2018, he worked as a study abroad student at the National University of Singapore (Jianping Xie's group). He studies on producing new alloy nanoclusters.

Kota Hamada

described above, these separation techniques are also often used to evaluate the distribution of a product and to track the reaction. Despite their importance, few reviews have focused on these techniques in the study of $Au_n(SR)_m$ clusters.[54]

This review summarizes research on the high-resolution separation of $Au_n(SR)_m$ and related clusters. In particular, we describe previous studies on PAGE, high-performance LC (HPLC), and thin-layer chromatography (TLC), which are separation techniques with high resolution and repeatability. The aim of this review is to provide a deep understanding of the features and usefulness of the three separation techniques through past research. The following section outlines the basic principles and experimental methods of PAGE, HPLC, and TLC. Then, in section 3, we briefly describe the previous high-resolution separation methods that were used before the appearance of these three techniques. Next, sections 4 to 6 outline previous studies on PAGE, HPLC, and TLC, respectively. Finally, section 7 summarizes the review and briefly describes future expectations.

2. Principles and procedure of each separation technique

2.1. Polyacrylamide gel electrophoresis

When a direct current flows through a solution, the charged sample in the solution moves in the direction of the oppositely charged electrode. A method of separating a substance based on this principle is called electrophoresis. In PAGE, substances move in a three-dimensional network consisting of polyacrylamide gel. Each metal cluster can be separated by this method because the mobility of the clusters differs depending on the charge, particle size, and shape. PAGE is generally used for the separation of hydrophilic $Au_n(SR)_m$ and its related clusters containing a ligand with a dissociable functional group.

In the experiment, first, a polyacrylamide-gel running layer is prepared between two plates using acrylamide and bis(acryl-

amide). Then, a polyacrylamide-gel stacking layer is prepared using acrylamide and bis(acrylamide) with a different concentration than that of the running layer. A sample solution containing several percent of glycerol is dropped on the upper end of the gel. Then, electrophoresis is performed by applying a voltage to the electrodes placed on the upper and lower sides of the gel. Each cluster is separated into several bands (Fig. 1A). Bands containing each metal cluster are cut out using a utility knife, and the clusters are eluted from the gel by leaving them in water and collecting them from the solution.

The device for PAGE is simple and inexpensive (Fig. 1A). In addition, when the cluster mixture is separated by PAGE, the separation of each component cluster can be visually confirmed. It is also possible to specify luminescent clusters by ultraviolet light irradiation. Moreover, PAGE is also useful for evaluating the product size and shape because the mobility of each metal cluster varies depending on the particle size and shape as well as the charge and the interaction with the solvent.

2.2. Liquid chromatography

Chromatography is a method used to separate a sample based on the difference in the extent of the interaction between the sample and the stationary phase. When the mobile phase is liquid, the technique is called LC.

2.2.1. Open column chromatography. For classical LC, the sample is loaded on the upper end of an open column with the stationary phase. Then, the mobile phase is passed through from the upper end of the column to separate the substances. Because of its simplicity, this method is often used for washing metal–SR complexes with greatly different sizes. However, there are almost no examples of $Au_n(SR)_m$ and their related clusters being separated with atomic precision because it is difficult to achieve a high degree of precision using this method. Therefore, this review does not introduce separation using this method.

2.2.2. High-performance liquid chromatography. When high pressure is applied in LC, the mobile phase passes

Sakiat Hossain: Postdoctoral researcher in the Negishi group at Tokyo University of Science. He obtained his B.Sc. (2005) from Ramakrishna Mission Residential College, Narendrapur, Calcutta University, M.Sc. (2007) from the Indian Institute of Technology Delhi, and Ph.D. (2013) from the Indian Institute of Technology Kanpur under the supervision of Prof. V. Chandrasekhar. He joined Tokyo University of Science in 2015. His research interests include the synthesis of novel metal clusters and study of their properties.

Sakiat Hossain

Tokuhisa Kawawaki: Assistant professor at the Department of Applied Chemistry at Tokyo University of Science. He received Ph.D. degree (2015) in applied chemistry from the University of Tokyo. Since 2016, he worked as a Japan Society for the Promotion of Science (JSPS) Postdoctoral fellow (PD) at the University of Melbourne. Since 2017, he worked as a JSPS super PD (SPD) at Kyoto University. In 2019, he moved to the current position. His current research topics include the synthesis of metal nanoparticles and nanoclusters in solution and their applications for photoelectrochemistry and photocatalysts.
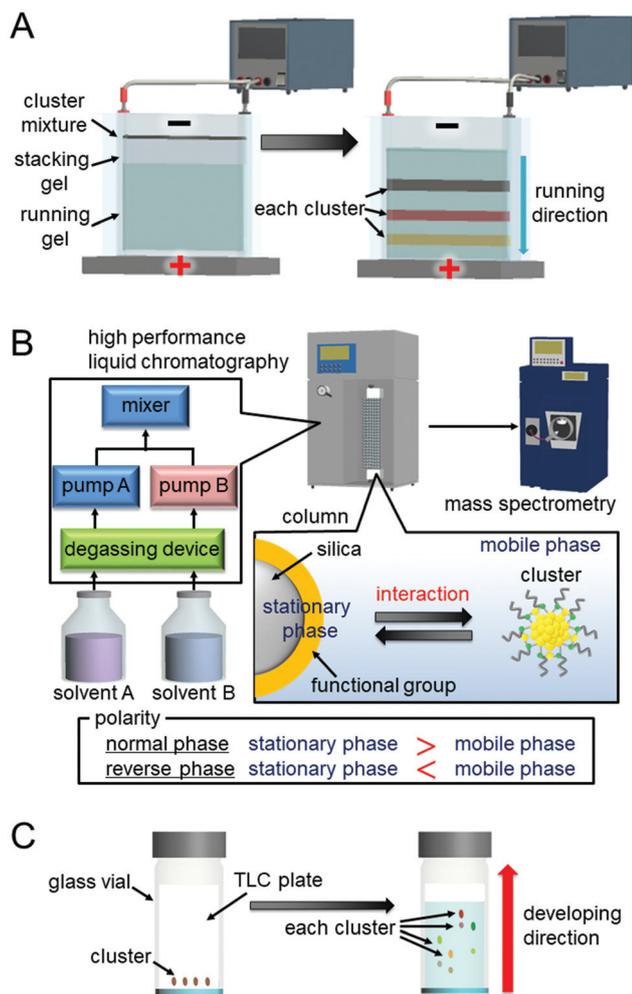
Tokuhisa Kawawaki

Fig. 1 Schematic illustration of (A) PAGE, (B) HPLC, and (C) TLC separation techniques.

through the column at a high flow rate. Consequently, the time during which the substance remains in the stationary phase is shortened, and the resolution and detection sensitivity are improved. This separation method is called HPLC to distinguish it from classical LC. The principle of separation used in HPLC is roughly divided into four types: adsorption, partition, ion exchange, and size exclusion. In addition, various other separation modes are used in actual HPLC analysis; however, these modes can be recognised as modifications or combinations of the above four separation principles in terms of the separation mechanism. The normal phase is the separation condition in which the polarity of the stationary phase is higher than that of the mobile phase. In contrast, reverse phase (RP) is the separation condition in which the polarity of the stationary phase is lower than that of the mobile phase (Fig. 1B). In the separation of $Au_n(SR)_m$ and their related clusters, partition, adsorption, and size exclusion have been used as the main separation principles.

The general HPLC system used for such separation consists of a mobile-phase solvent reservoir, a degasser device, a high-

pressure liquid pump, an injector, a column, and a detector (Fig. 1B). There are two types of mobile phases, one using a single mobile phase and the other using multiple types of mobile-phase solvents while arbitrarily changing their volume ratio. The first method is called the isocratic mode, and the second method is called the gradient mode. In general, a column is produced by filling a stainless-steel tube with a particulate stationary phase (column filler) at high pressure and sealing its upper and lower ends with a sintered porous stainless filter. Silica gel particles with surfaces modified by an organic layer are often used as the column filler (Fig. 1B).

HPLC has advantages of resolution and repeatability. There is also the advantage that electrospray ionization (ESI) mass spectrometry (MS) can be used for the detection. As opposed to separation by PAGE, when the HPLC apparatus and ESI mass spectrometer are directly connected (LC/MS), all the generated clusters can be directly led to the MS section. Thus, it is possible to determine the chemical composition of very minor components that cannot be detected by PAGE.

2.2.3. Thin-layer chromatography. There have been some reports on the separation of $Au_n(SR)_m$ clusters by TLC using a planar stationary phase in recent years. The TLC plates are prepared by coating a stationary phase on a flat glass, aluminium, or plastic plate. Currently, TLC plates coated with various types of stationary phases are commercially available. The separation principles of adsorption, partition, ion exchange, and size exclusion can also be used in TLC separation.

In the experiment, the solution containing the sample is spotted 15 to 25 mm above the lower end of the TLC plate using a micropipette or a capillary tube. After drying the sample, the plate is allowed to stand with the spot facing down in a sealed container with a solvent (the mobile phase). The sample is separated by rising of the solvent from the lower side *via* capillary action (Fig. 1C). The band containing each $Au_n(SR)_m$ cluster is cut out with a spatula, and each $Au_n(SR)_m$ cluster is collected from the plate.

With TLC, it is difficult to achieve the same degree of resolution as HPLC. However, TLC is a less expensive and it uses simpler experimental apparatus than HPLC. Therefore, when the distances that each $Au_n(SR)_m$ cluster travel on the plate are significantly different, the target $Au_n(SR)_m$ cluster can be easily and inexpensively isolated using this method. It is also one of the advantages of this method that the separation of $Au_n(SR)_m$ clusters can be visually confirmed, as for PAGE.

3. Early studies on separation

Many attempts were made to separate $Au_n(SR)_m$ clusters based on the number of constituent atoms before the use of the above three methods (PAGE, HPLC, and TLC).[34–38] For example, Whetten *et al.* synthesized $Au_n(SC_lH_{2l+1})_m$ clusters (SC_lH_{2l+1} = alkanethiolate) as a ligand. They gradually added a poor solvent and precipitated clusters from large to small in order.[35] In these studies, each separated $Au_n(SC_lH_{2l+1})_m$ cluster was evaluated mainly using matrix-assisted laser desorption/
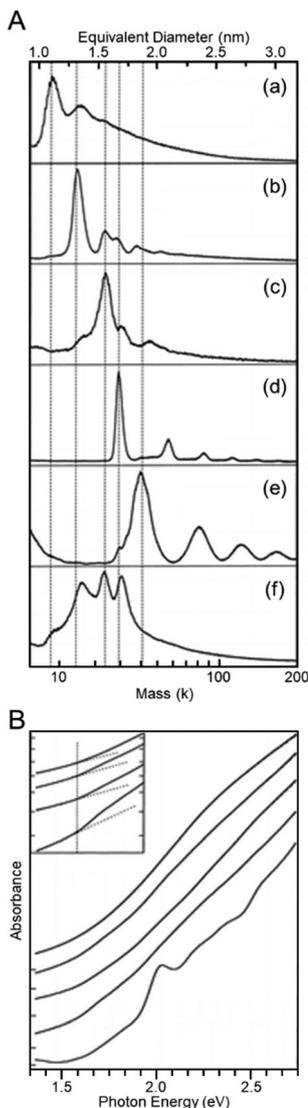
Fig. 2 (A) MALDI mass spectra of $Au_n(SC_lH_{2l+1})_m$ clusters with different core sizes (l = 6, 12, or 18); (a) 8, (b) 14, (c) 22, (d) 28, and (e) 34–38 kDa clusters. (f) Crude sample of $Au_n(SC_{12}H_{25})_m$ clusters. (B) Optical absorption spectra of $Au_n(SC_lH_{2l+1})_m$ clusters with different core sizes: (bottom to top) 8, 14, 22, 28, and 34–40 kDa clusters. Reproduced with permission from ref. 35. Copyright 1997 American Chemical Society.

ionization (MALDI)-MS. In the mass spectrum of each $Au_n(SC_lH_{2l+1})_m$ cluster, ion peaks appeared in different mass regions (Fig. 2A), which indicated that the $Au_n(SC_lH_{2l+1})_m$ clusters were separated based on their size. Unfortunately, these mass spectra included only the fragmentation peaks of each $Au_n(SC_lH_{2l+1})_m$ cluster.[38] Therefore, the chemical composition of each $Au_n(SC_lH_{2l+1})_m$ cluster was not accurately determined at this stage. Murray *et al.* also separated $Au_n(SR)_m$ clusters (SR = SC_lH_{2l+1} or SC_2H_4Ph; SC_2H_4Ph = phenylethanethiolate) using solvent-selective extraction.[55] Although this method has been revealed to be useful for obtaining each stable $Au_n(SR)_m$ cluster at atomic resolution in the later studies[56–58] and thereby often used for the isolation of $Au_n(SR)_m$ clusters in large quantities

in recent studies,[59–63] unfortunately, the separated $Au_n(SR)_m$ clusters could not be confirmed to be isolated at atomic resolution at this stage. However, these studies provided considerable information on the correlation between the particle size and electronic structure in the $Au_n(SR)_m$ clusters (Fig. 2B).[34–38] Since then, the separation technique for $Au_n(SR)_m$ clusters has progressed rapidly with the introduction of separation methods offering high resolution and repeatability and the improvement of mass spectrometers.

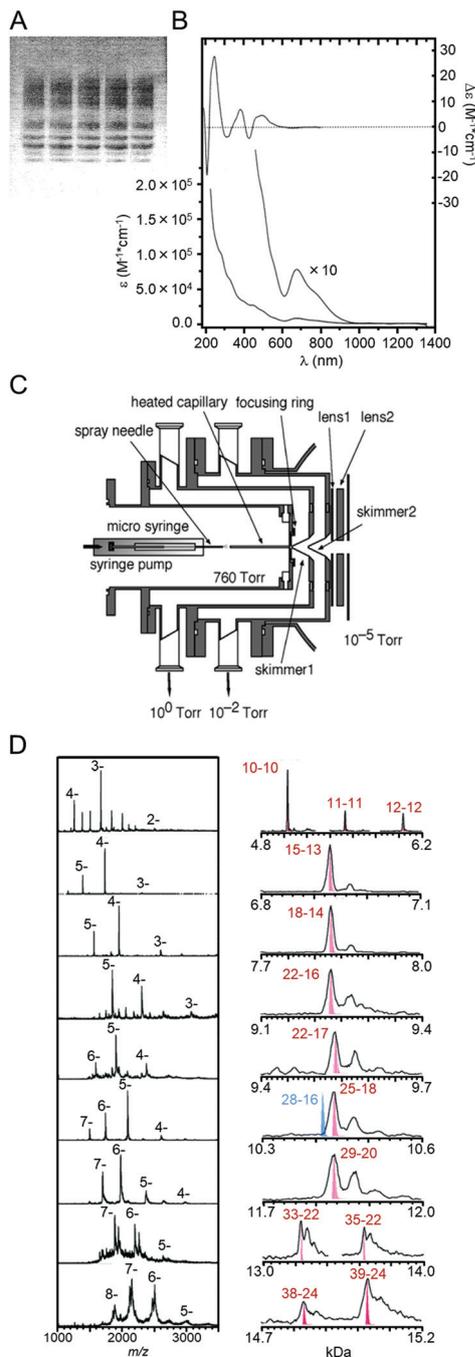## 4. PAGE separation

4.1. PAGE separation for isolation

PAGE was first applied to separate $Au_n(SR)_m$ clusters in 1998. Schaaf and Whetten *et al.* separated $Au_n(SG)_m$ clusters (SG = glutathionate) into multiple bands using PAGE (Fig. 3A).[64] For the separation, they made gels in higher concentration (~40%) than the gels used in protein separations. This optimization of the gel concentration led to the high-resolution separation of $Au_n(SG)_m$ clusters (Fig. 3B). They also measured the $Au_n(SG)_m$ clusters in each band using MALDI-MS and ESI-MS. However, these measurements did not provide mass spectra with a high signal/noise (S/N) ratio. Therefore, at this stage, the chemical composition of each separated $Au_n(SG)_m$ cluster had not been accurately determined.

Later, Negishi and Tsukuda *et al.* demonstrated that this method could be used to separate a mixture into each $Au_n(SG)_m$ cluster with atomic precision.[41,65] They evaluated the chemical compositions of the $Au_n(SG)_m$ cluster contained in each band using their homemade ESI mass spectrometer. Using their homemade apparatus, an ionized solvent containing $Au_n(SG)_m$ clusters could be efficiently introduced into the mass spectrometer (Fig. 3C).[41,65] As a result, a high S/N ratio was achieved in the mass spectra, and the separated $Au_n(SG)_m$ clusters were assigned as $Au_{10–12}(SG)_{10–12}$, $Au_{15}(SG)_{13}$, $Au_{18}(SG)_{14}$, $Au_{22}(SG)_{16}$, $Au_{22}(SG)_{17}$, $Au_{25}(SG)_{18}$, $Au_{29}(SG)_{20}$, $Au_{33}(SG)_{22}$, and $Au_{39}(SG)_{24}$, respectively (Fig. 3D). This study also clarified that $Au_{25}(SG)_{18}$ is especially stable.[65] Stable clusters with similar absorption spectra had previously been reported by Whetten *et al.* and Murray *et al.*[66,67] This study revealed that the exact chemical composition of these clusters was $Au_{25}(SR)_{18}$.

For the $Au_n(SG)_m$ clusters, Kimura *et al.* and Dass *et al.* separated larger-sized clusters up to $Au_{\sim56}(SG)_{\sim29}$ and $Au_{43}(SG)_{26}$, respectively.[68,69] In Dass's study, the chemical composition of each cluster was determined using a commercially available mass spectrometer.[69] The detection sensitivity of commercial apparatuses has improved, and in research since 2008, the chemical composition of separated clusters has been evaluated using commercial rather than homemade apparatuses.
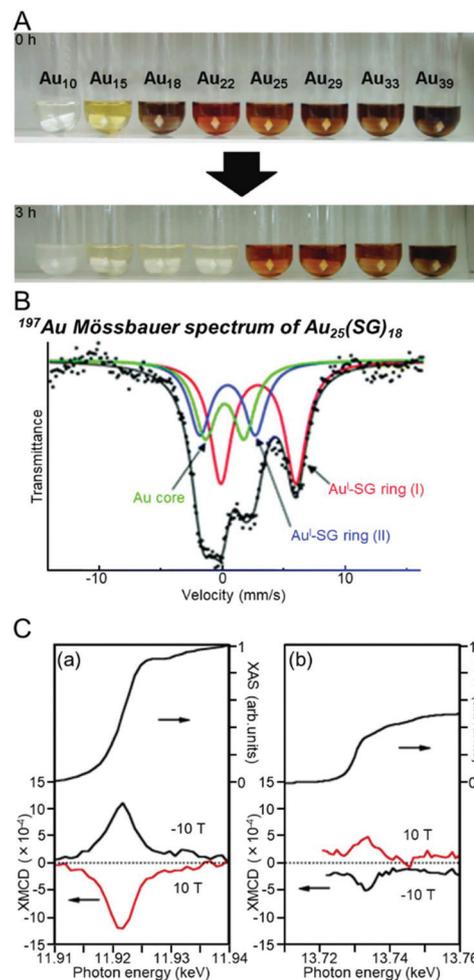
The isolation of $Au_n(SG)_m$ clusters with atomic precision enabled a deep understanding of the stability, structure, and other properties of $Au_n(SG)_m$ clusters to be obtained. Tsukuda and Teranishi *et al.* showed that a series of $Au_n(SG)_m$ clusters exhibited especially high stability against etching using excess thiol (Fig. 4A)[39] and that $Au_{25}(SG)_{18}$ could be selectively synthesized in a solution where etching is likely to occur.[44]

Fig. 3 (A) PAGE separation of $Au_n(SG)_m$ clusters and (B) optical absorption spectra of the main product in the sample in (A) from an early study.[64] (C) ESI source constructed in the study of ref. 41. (D) ESI mass spectrum of each fraction separated by PAGE.[41] Reproduced with permission from ref. 64 and 41. Copyright 1998 American Chemical Society and Copyright 2005 American Chemical Society.

Fig. 4 (A) Photographs of a series of $Au_n(SG)_m$ cluster aqueous solutions (n = 10, 15, 18, 22, 25, 29, 33, and 39) before and after a 3 h etching reaction.[39] (B) Mössbauer spectrum of $Au_{25}(SG)_{18}$.[70] (C) X-ray absorption spectra (top) and XMCD (bottom) spectra of $Au_{18}(SG)_{14}$ at the (a) Au L$_3$ and (b) Au L$_2$ edges with an applied magnetic field of 10 T at 2.7 K.[42] Reproduced with permission from ref. 39, 70 and 42. Copyright 2007 Wiley-VCH, Copyright 2007 American Chemical Society, and Copyright 2006 American Chemical Society.

Kojima and Tsukuda *et al.* experimentally demonstrated using ^{197}Au Mössbauer spectroscopy that $Au_n(SR)_m$ clusters have a geometrical structure in which a Au core is covered by Au(ɪ)–SR oligomers (Fig. 4B), which had been predicted by density functional theory (DFT) calculations.[70] Tsukuda and Yokoyama *et al.* showed that fine $Au_n(SG)_m$ clusters could exhibit magnet-

ism using X-ray magnetic circular dichroism (XMCD) spectrometry (Fig. 4C).[42] Unfortunately, the interpretations in these studies were not necessarily accurate. The exact geometrical structure of $Au_{25}(SC_2H_4Ph)_{18}$ was later determined using SC-XRD by Murray *et al.* and Jin *et al.*, independently.[56,71] Jin *et al.* clarified the exact origin of the magnetism using electron spin resonance spectroscopy.[72] However, studies on a series of isolated $Au_n(SG)_m$ clusters by Tsukuda *et al.* have provided many new insights into the stability, electronic/geometrical structures, and other properties of $Au_n(SR)_m$ clusters. These findings further demonstrate that it is essential to conduct research on fine metal clusters with controlled chemical composition to elucidate their fundamental properties.

Separation using PAGE has also been applied for the isolation of $Au_n(SR)_m$ clusters protected with other hydrophilic ligands. Negishi and Tsukuda *et al.* separated tiopronin
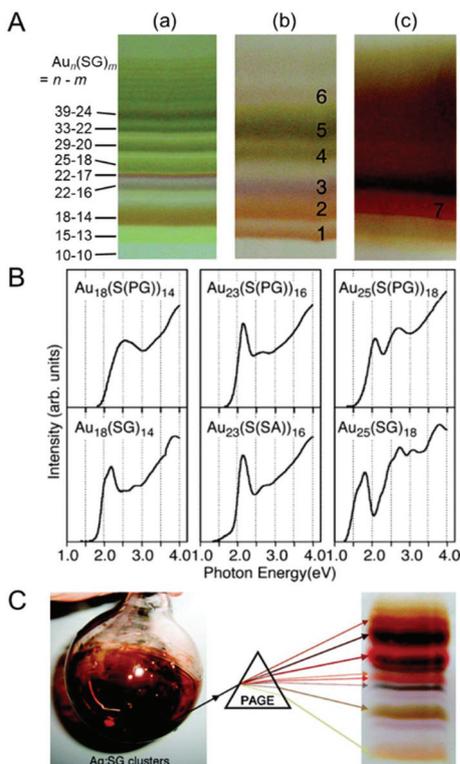
Fig. 5 (A) PAGE separation of (a) $Au_n(SG)_m$, (b) $Au_n(S(PG))_m$, and (c) $Au_n(S(SA))_m$ clusters.[73] (B) Comparison of optical absorption spectra of $Au_{18}(SR)_{14}$, $Au_{23}(SR)_{16}$, and $Au_{25}(SR)_{18}$ with different ligand structures.[73] (C) PAGE separation of $Ag_n(SG)_m$ clusters.[79] Reproduced with permission from ref. 73 and 79. Copyright 2006 American Chemical Society and Copyright 2010 American Chemical Society.

(S(PG))- or mercaptosuccinic acid (S(SA))-protected Au clusters using PAGE (Fig. 5A).[73] They showed that the chemical compositions of the isolated $Au_n(SR)_m$ clusters differed depending on the ligand structure by comparing the chemical compositions of $Au_n(S(PG))_m$, $Au_n(S(SA))_m$, and $Au_n(SG)_m$ clusters.[73] Comparison of the optical absorption spectra of these clusters with the same chemical composition revealed that the electronic structure of $Au_n(SR)_m$ clusters also changes depending on the ligand structure (Fig. 5B).[73] Tsukuda et al. isolated $Au_{25}(S(PG))_{18}$ in high purity and obtained information on its geometrical structure in a later study.[74] In addition, other hydrophilic $Au_n(SR)_m$ clusters were separated using PAGE by Bürgi et al. (SR = N-isobutyl-cysteine)[75,76] and Yao et al. (SR = penicillamine (Pen)[77] and 3-mercaptophenyl-boronic acid[78]).

Separation using PAGE has also been applied for the isolation of other metal clusters. Bigioni et al. separated $Ag_n(SG)_m$ clusters using PAGE (Fig. 5C) and suggested that $Ag_n(SG)_m$ clusters could have a different chemical composition than $Au_n(SG)_m$ clusters by comparing each gel.[79] The main product of $Ag_n(SG)_m$ clusters was later determined to be $Ag_{32}(SG)_{19}$ by Griffith and Bigioni et al.,[80] and this chemical composition actually cannot be observed for $Au_n(SG)_m$ clusters.

Pradeep et al. separated $Ag_n(SG)_m$ clusters and showed that $Ag_{32}(SG)_{19}$ exhibits strong photoluminescence (PL).[81] Yao and

Kimura et al. separated $Ag_n(D/L\text{-}Pen)_m$ clusters and revealed that they have higher mobility than $Au_n(Pen)_m$ clusters.[82] They concluded that the mobility differences originated from the larger surface charge of the $Ag_n(D/L\text{-}Pen)_m$ clusters.[82]

In this way, it is possible to isolate SR-protected metal clusters composed of various ligands and metal elements with atomic precision using PAGE.[83–101] By conducting research on a series of separated clusters, much knowledge has been obtained on the chemical composition and stability, electronic/geometrical structure, and physical properties of various SR-protected metal clusters.

4.2. PAGE separation for reaction control

In section 4.1, we introduced the isolation of metal clusters by PAGE. Meanwhile, fine metal clusters often exhibit a colour that depends on the number of constituent atoms. Thus, when they are separated by PAGE, the distribution of their chemical compositions can be confirmed visually. For this reason, PAGE is also often used to examine the distribution of chemical compositions of a product, optimize reaction conditions, elucidate the degraded processes, and track reactions.[102–110]

For example, Tsukuda and Teranishi et al. observed that $Au_{25}(SG)_{18}$ was a major product when a triphenylphosphine (PPh₃)-protected Au cluster was mixed with glutathione (GSH). They attempted to optimize the reaction conditions to selectively synthesize such a stable cluster with atomic precision. In this experiment, the distribution of the product under each experimental condition was first checked by PAGE separation (Fig. 6A)[44] and then estimated by ESI-MS in the final stage. The results indicated that high-purity $Au_{25}(SG)_{18}$ was present in the product (Fig. 6B).[44] Later, they mixed a series of $Au_n(SG)_m$ clusters with GSH and traced the etching process using PAGE and discussed why $Au_{25}(SG)_{18}$ was selectively synthesized in the reaction between the PPh₃-protected Au cluster and GSH.[39]

Ackerson et al. synthesized $Au_{102}(p\text{-}MBA)_{44}$ (p-MBA = p-mercaptobenzoic acid) under different gas atmospheres and examined the distribution of products using PAGE. They observed that O_2 was required as a gas for radical generation when
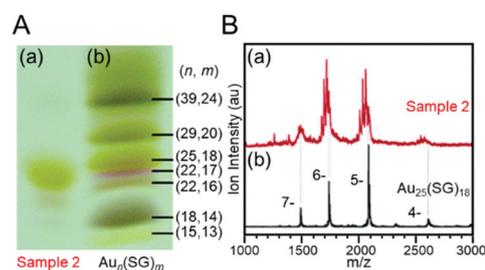
Fig. 6 (A) PAGE photograph of (a) $Au_{25}(SG)_{18}$ obtained by size focusing (sample 2) and (b) a series of $Au_n(SG)_m$ clusters. (B) Comparison of the ESI mass spectrum of (a) $Au_{25}(SG)_{18}$ obtained by size focusing and (b) $Au_{25}(SG)_{18}$ isolated by PAGE separation. The progression of the mass peaks in the spectrum of sample 2 results from the partial hydrolysis of the SG ligands. Reproduced with permission from ref. 44. Copyright 2005 American Chemical Society.
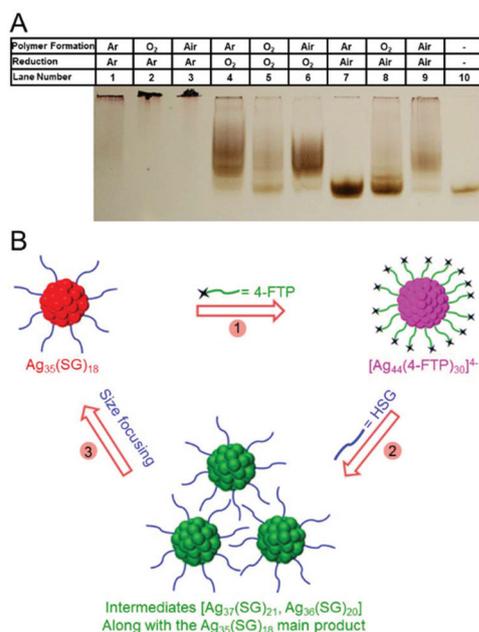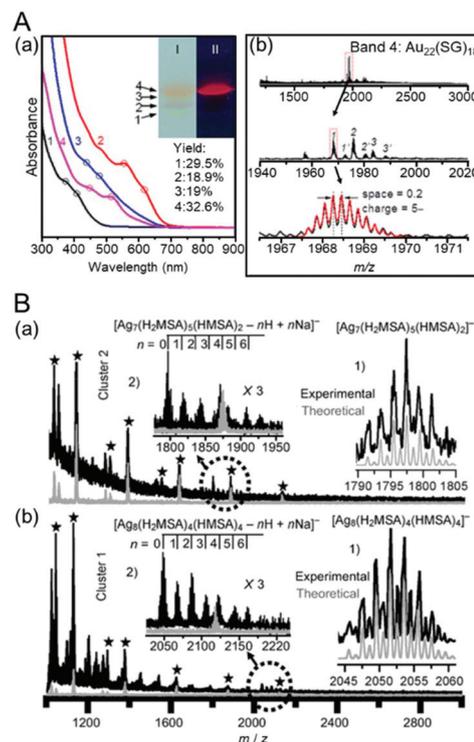
Fig. 7 (A) Effect of atmosphere on $Au_{102}(p\text{-MBA})_{44}$ synthesis. Crossover experiments showing the effect of oxygenated *vs.* inert atmosphere on the synthesis of $Au_{102}(p\text{-MBA})_{44}$. Lane 10 is a sample of pure $Au_{102}(p\text{-MBA})_{44}$ for reference. The PAGE conditions were 20% acrylamide at 125 V for 2 h.[111] (B) Schematic illustration of reversible transformation (Steps 1–3) of $Ag_{35}(SG)_{18}$ into $Ag_{44}(4\text{-FTP})_{30}$.[112] Reproduced with permission from ref. 111 and 112. Copyright 2016 American Chemical Society. Copyright 2015 American Chemical Society.

Fig. 8 (A) (a) Optical absorbance spectra of Au NCs separated from bands 1–4 in native PAGE gel. The inset shows photographs of the PAGE separation (lane I) before and (lane II) after UV light irradiation. (b) ESI mass spectra of species 4. The red lines are the simulated isotope pattern of $[Au_{22}(SG)_{18}{}^{0}-5H]^{5-}$.[43] (B) Negative-ion MALDI (black) and LDI (gray) mass spectra of (a) $Ag_{7}(S(SA))_{7}$ and (b) $Ag_{8}(S(SA))_{8}$.[117] Reproduced with permission from ref. 43 and 117. Copyright 2014 American Chemical Society and Copyright 2010 Wiley-VCH.

using an organic solvent during the synthesis (Fig. 7A).[111] They also showed that $Au_{102}(p\text{-MBA})_{44}$ could be synthesized under an argon atmosphere by adding a radical initiator to the reaction vessel. Bigioni *et al.* observed the degradation process of $Ag_n(SG)_m$ clusters under various conditions (time, pH, presence or absence of salt, *etc.*) using PAGE. These studies revealed that the degradation of the $Ag_n(SG)_m$ clusters can be relatively suppressed by adjusting the pH of the solution to near neutral or by adding Ag^+ ions into the solution.[40] Bakr *et al.* demonstrated using PAGE that the structural changes between $Ag_{35}(SG)_{18}$ and $Ag_{44}(4\text{-FTP})_{30}$ (4-FTP = 4-fluorothiophenolate) induced by ligand exchange are reversible (Fig. 7B).[112] Xie *et al.* revealed that $Au_{18}(SG)_{14}$ could be produced as an intermediate in the synthesis of $Au_{22}(SG)_{18}$ with carbon monoxide (CO) reduction by monitoring the reaction using PAGE.[113]

In this way, the use of PAGE enables the chemical composition distribution of the product to be clarified. Through the use of such PAGE separation, much knowledge has been obtained on appropriate synthesis conditions, stable conditions, and reaction mechanisms.

4.3. PAGE separation to identify luminescent cluster

Fine noble metal clusters often exhibit PL.[114,115] Au and Ag are harmless elements, unlike cadmium and arsenic, which form compound semiconductors with strong emission.[116] However,

it is not easy to identify a metal cluster that emits PL with high quantum yield from a mixture. If the mixture is separated by PAGE and then the gel is irradiated with ultraviolet light, it is possible to visually identify the metal cluster exhibiting PL. Therefore, PAGE has often been utilized to identify luminescent metal clusters.

$Au_{22}(SG)_{18}$, which emits red light with high quantum yield (~8%), was identified by such PAGE separation.[43] Xie *et al.* synthesized $Au_n(SG)_m$ clusters using CO as the reduction agent and separated the mixture into each band using PAGE. The products were separated into four different $Au_n(SG)_m$ clusters. Irradiation of the obtained gel with ultraviolet light revealed that $Au_{22}(SG)_{18}$, which has the lowest mobility, emits strong red PL (Fig. 8A). Based on the results of DFT calculation and X-ray absorption spectroscopy, they suggested that $Au_{22}(SG)_{18}$ has a geometrical structure in which the Au core is covered by a longer Au(I)–SG staple (RS–$[Au\text{–}SR]_n$; n = 3, 4), which differs from the structure of other $Au_n(SG)_m$ clusters. They concluded that $Au_{22}(SG)_{18}$ emits PL with high quantum yield because of the aggregation excitation emission effect caused by the long Au(I)–SG staple. Pradeep *et al.* succeeded in finding $Ag_7(S(SA))_7$ that emits red PL and $Ag_8(S(SA))_8$ that emits blue PL using PAGE separation (Fig. 8B).[117]

4.4. PAGE separation for structural estimation

In PAGE separation, the mobility of each metal cluster depends on the particle size and shape as well as its charge and interaction with the solvent. Thus, there are several examples of the use of PAGE for structural and shape evaluation of $Au_n(SR)_m$ clusters.

Ackerson *et al.* synthesized $Au_n(p\text{-MBA})_m$ clusters with unknown size and estimated their chemical compositions from their PAGE mobility. In their study, they first ran $Au_{102}(p\text{-MBA})_{44}$ and $Au_{144}(p\text{-MBA})_{60}$ with known chemical composition through a gel and estimated the correlation between their mobility and chemical composition. Then, $Au_n(p\text{-MBA})_m$ clusters with unknown size were run through a gel at the same concentration, and the chemical composition was estimated to be $Au_{\sim230}(p\text{-MBA})_{\sim88}$ from the mobility and the aforementioned correlation.[118] Lehtovaara, Häkkinen, and Pettersson *et al.* demonstrated by PAGE separation that mixing $Au_{102}(p\text{-MBA})_{44}$ or $Au_{\sim250}(p\text{-MBA})_n$ with biphenyl-4,4′-dithiol causes ligand exchange, resulting in the multimerization of $Au_{102}(p\text{-MBA})_{44}$ or $Au_{\sim250}(p\text{-MBA})_n$ (Fig. 9).[119]

4.5. Sodium dodecyl sulfate-PAGE separation

In the PAGE separation described thus far, not only the molecular weight of the cluster but also the charge state was reflected in the mobility. Therefore, to more accurately estimate the correlation between the chemical composition and mobility, it is necessary to exclude the effect of the charge state. Adding sodium dodecyl sulfate (SDS) to the sample solution and electrophoresis solution results in an almost constant charge-to-size ratio of the cluster, eliminating the effect of the charge state on the mobility. Such a SDS-PAGE solution is used in protein separation.[120]

Cheng and Häkkinen *et al.* used SDS-PAGE for the separation of $Au_n(SR)_m$ clusters.[121] They replaced some ligands of $Au_{102}(p\text{-MBA})_{44}$ with maleimide (C_6MI) to bind $Au_{102}(p\text{-MBA})_{44}$ efficiently to a nanocapsid. They confirmed using SDS-PAGE that the $Au_{102}(p\text{-MBA})_{44-x}(C_6MI)_x$ bound to the nanocapsid with higher efficiency than the unreacted $Au_{102}(p\text{-MBA})_{44}$.
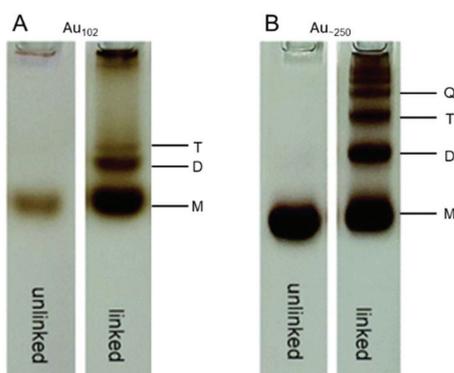
5. HPLC separation

As with PAGE, there have been many reports on the separation of $Au_n(SR)_m$ and related clusters using HPLC.[122–145] The main separation methods include RP partition chromatography, ion-pair chromatography, hydrophilic interaction liquid chromatography, size exclusion chromatography, and chiral chromatography (Fig. 10). In the following, research examples are introduced.

5.1. Reverse phase partition chromatography

RP partition chromatography provides ease of handling and has many stationary phases with a high number of theoretical plates. Furthermore, this method also facilitates the use of LC/MS because the mobile phase used in this chromatography technique is suitable for the ionization of the cluster in ESI-MS. Because of these advantages, more than 80% of HPLC analysis uses an RP column.

In RP partition chromatography, the polarity of the stationary phase is lower than that of the mobile phase (Fig. 1B). Under this condition, the solute is in partition equilibrium between the stationary and mobile phases, and each solute is separated by a difference in the partition coefficient. In this chromatography method, silica gel supports chemically modified with an octadecyl group (C18), an octyl group (C8), a phenyl group (Ph), *etc.* are used as the stationary phase (Fig. 11A).

5.1.1. Separation of clusters by cluster size. Murray *et al.* first attempted to separate $Au_n(SR)_m$ clusters using RP partition chromatography. In 2003, they synthesized a mixture of $Au_n(SC_6H_{13})_m$ clusters (SC_6H_{13} = hexanethiolate) and attempted to separate each cluster using a C8 column.[146] The $Au_n(SR)_m$ clusters with metal cores of approximately 1.5 nm were separated into multiple peaks (Fig. 12A). They estimated the size of $Au_n(SC_6H_{13})_m$ clusters contained in each fraction using methods such as optical absorption spectroscopy and electrochemical measurements and showed that smaller clus-
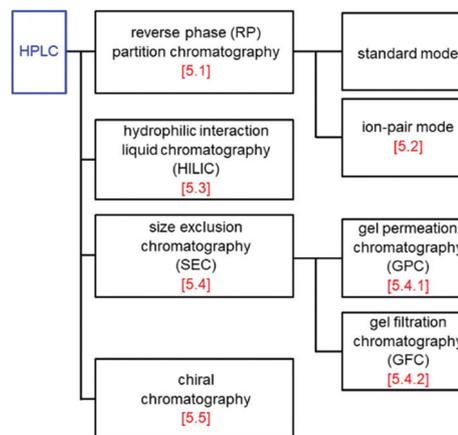

Fig. 9 (A) and (B) PAGE bands of $Au_{102}(p\text{-MBA})_{44}$ and $Au_{\sim250}(p\text{-MBA})_n$ clusters and their linked multimers. Reproduced with permission from ref. 119. Copyright 2016 The Royal Society of Chemistry.
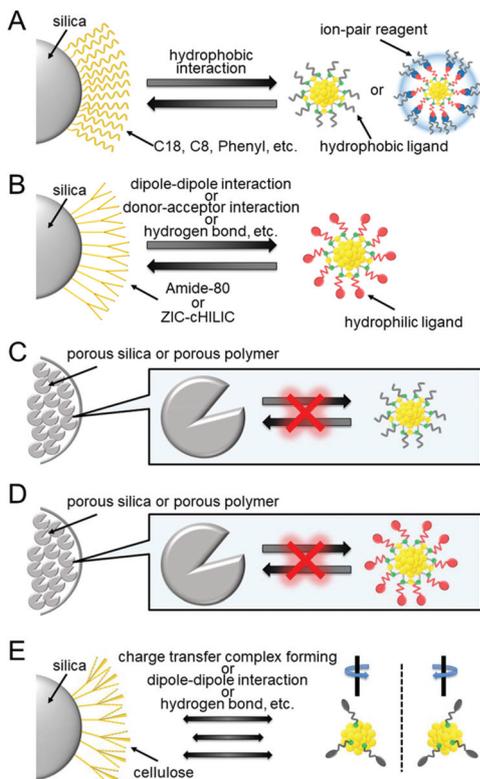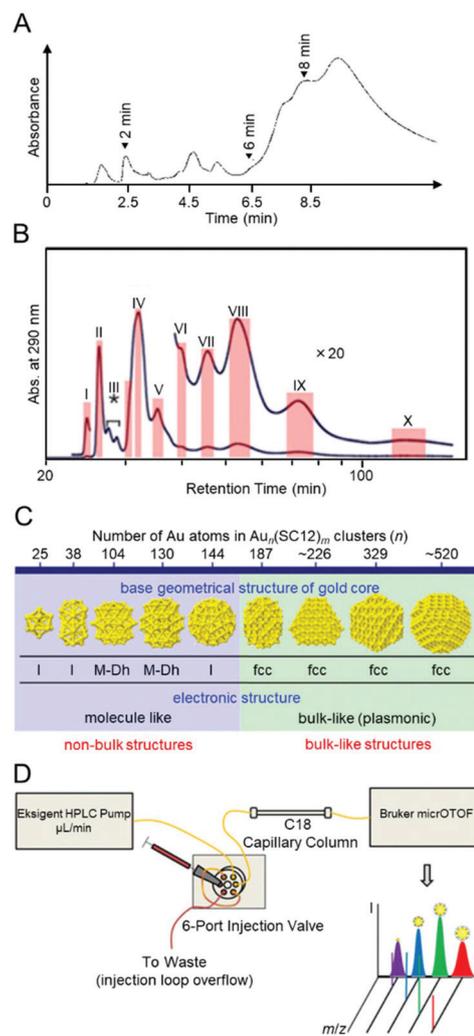

Fig. 10 Classification of HPLC used in the study of SR-protected metal clusters. The number in square brackets is the section number.

Fig. 11 Schematic illustration of the solid phase used in each chromatography technique: (A) RP partition and ion-pair chromatography, (B) HILIC, (C) GPC, (D) GFC, and (E) chiral chromatography.

Fig. 12 Separation of $Au_n(SR)_m$ clusters by RP partition chromatography. (A) Chromatogram of the as-prepared $Au_n(SC_6H_{13})_m$ clusters obtained using a C8 column by the Murray group.[146] (B) Chromatogram of the as-prepared $Au_n(SC_{12}H_{25})_m$ clusters obtained using two connected columns (C8 and Ph).[154] (C) Critical size for emergence of non-bulk electronic and geometrical structures in $Au_n(SC_{12}H_{25})_m$ clusters elucidated by studies on a series of isolated $Au_n(SC_{12}H_{25})_m$ clusters.[154] (D) Schematic illustration of capillary liquid chromatography mass spectrometry (LC/MS) used in the study of $Au_n(SC_2H_4Ph)_m$ clusters.[160] Reproduced with permission from ref. 146, 154, and 160. Copyright 2003 American Chemical Society, Copyright 2015 American Chemical Society, and Copyright 2016 American Chemical Society.

ters eluted at shorter retention times.[147,148] The cluster included in the earliest eluting peak was assigned to Au_{38}, and that included in the second eluting peak was assigned to Au_{140}. The researchers also observed that connecting a C8 column to a Ph column improved the resolution. They succeeded in separating Au_{140} and Au_{225}, which has a larger metal core, using such a connected column.[149]

Negishi *et al.* succeeded in separating a series of $Au_n(SC_{12}H_{25})_m$ clusters ($SC_{12}H_{25}$ = dodecanethiolate) depending on the number of constituent atoms using such a connected column. Four distinct peaks were observed in the chromatogram, corresponding to $Au_{102}(SC_{12}H_{25})_{44}$, $Au_{130}(SC_{12}H_{25})_{50}$, $Au_{144}(SC_{12}H_{25})_{60}$, and $Au_{187}(SC_{12}H_{25})_{68}$, respectively.[150] Although the isolation of $Au_{102}(SR)_{44}$ and $Au_{144}(SR)_{60}$ had been previously reported,[101,151] $Au_{130}(SR)_{50}$ and $Au_{187}(SR)_{68}$ clusters were successfully isolated for the first time in this experiment.[152,153] They also succeeded in finding an experimental condition for separating $Au_n(SC_{12}H_{25})_m$ clusters in a wide range from $Au_{38}(SC_{12}H_{25})_{24}$ to $Au_{\sim520}(SC_{12}H_{25})_{\sim130}$ at the same time (Fig. 12B).[154] In cooperation with Häkkinen and Tsukuda *et al.*, they clarified the electronic and geometrical structures of a series of isolated $Au_n(SC_{12}H_{25})_m$ clusters and concluded that the transition from bulk to non-bulk occurs in the region from $Au_{187}(SC_{12}H_{25})_{68}$ to $Au_{144}(SC_{12}H_{25})_{60}$ in the $Au_n(SC_{12}H_{25})_m$ clusters (Fig. 12C).[154] Regarding this transition,

the recent studies by Jin *et al.*[155,156] and Dass *et al.*[157,158] revealed that the transition from bulk to non-bulk occurs between $Au_{279}(SR)_{84}$ to $Au_{246}(SR)_{80}$ in the case of $Au_n(SR)_m$ clusters including benzenethiolate in the functional group of the ligand. Knoppe *et al.* also studied the separation of these $Au_n(SC_{12}H_{25})_m$ clusters. They found the conditions for separating $Au_{25}(SC_{12}H_{25})_{18}$ and $Au_{38}(SC_{12}H_{25})_{24}$ with high resolution and revealed the correlation between the alkyl chain length and retention time through experiments conducted under such conditions.[159]

Black and Whetten *et al.* separated $Au_n(SC_2H_4Ph)_m$ clusters using a capillary C18 column. Their use of a capillary column was unique, enabling suppression of the quantity of the mobile phase and thereby direct evaluation of the chemical composition of the eluted cluster with a directly connected ESI mass spectrometer (Fig. 12D).[160,161] They also succeeded in clearly separating $Au_{104}(SC_2H_4Ph)_{45}$, $Au_{130}(SC_2H_4Ph)_{50}$, $Au_{137}(SC_2H_4Ph)_{56}$, and $Au_{144}(SC_2H_4Ph)_{60}$ using a similar method.[161]

5.1.2. Separation of clusters by charge state. As described above, in RP partition chromatography, each solute can be separated by the difference in the partition coefficient in the column. Because the charge state of the solute greatly affects the partition coefficient, separating $Au_n(SC_2H_4Ph)_m$ clusters with different charge states can be easily achieved using RP partition chromatography.

Negishi *et al.* reported that $[Au_{25}(SC_{12}H_{25})_{18}]^0$ and $[Au_{25}(SC_{12}H_{25})_{18}]^-$ elute at significantly different retention times in RP partition chromatography (Fig. 13). In this study, they estimated the charge state of $Au_{24}Pd(SC_{12}H_{25})_{18}$ with an unknown charge state by comparing the retention time of $Au_{24}Pd(SC_{12}H_{25})_{18}$ with that of $[Au_{25}(SC_{12}H_{25})_{18}]^0$ and $[Au_{25}(SC_{12}H_{25})_{18}]^-$. This comparison elucidated that $Au_{24}Pd(SC_{12}H_{25})_{18}$ could be synthesized in the neutral form ($[Au_{24}Pd(SR)_{18}]^0$).[162] They also demonstrated by a similar comparison that $Au_{25-x}Ag_x(SC_{12}H_{25})_{18}$ could be synthesized in the negative form ($[Au_{25-x}Ag_x(SR)_{18}]^-$).[163] Their interpretation was later confirmed by the SC-XRD analysis of $Au_{24}Pd(SR)_{18}$ and $Au_{25-x}Ag_x(SR)_{18}$ ($SR = SC_2H_4Ph$).[164,165]

5.1.3. Separation of clusters by ligand combination. The physical and chemical properties of $Au_n(SR)_m$ clusters vary depending on the ligand type in addition to the core size. For example, the solubility in a solvent and the quantum yield of PL[166] vary depending on the functional group of the ligand. When a SR with a specific function is used as the ligand, it is possible to provide a specific function, such as molecular recognition ability[167] or catalytic ability, to the $Au_n(SR)_m$ clusters. Thus, controlling the ligand composition is an extremely effective way to control the function of the cluster. If it were possible to substitute only a limited number of ligands with other SRs, strict control of the function of metal clusters might be possible as well as regular arrangement of metal clusters on the substrate. However, when $Au_n(SR)_m$ clusters are synthesized using multiple types of SRs, the product typically has a distribution in the ligand combination.[168–170] Therefore, to realize strict control of functions and precise arrangement of clusters, it is necessary to separate the obtained mixture at high resolution depending on the ligand combination. Using RP partition chromatography, it is also possible to separate $Au_n(SR_1)_{m-x}(SR_2)_x$ clusters with two types of ligands (SR_1 and SR_2) depending on the ligand combination.

Negishi and Pradeep *et al.* reported that multiple ligands of $Au_{24}Pd(SC_{12}H_{25})_{18}$ can be exchanged with SBB (4-*tert*-butylbenzenemethanethiolate) *via* the reaction of $Au_{24}Pd(SC_{12}H_{25})_{18}$ with 4-*tert*-butylbenzenemethanethiol (BBSH) in solution. However, the obtained cluster had a distribution in the number of exchanged ligands. They succeeded in separating such a mixture depending on ligand composition using RP partition chromatography.[171] In this experiment, first, all the $Au_{24}Pd(SC_{12}H_{25})_{18-x}(SBB)_x$ was adsorbed on the stationary phase. Then, $Au_{24}Pd(SC_{12}H_{25})_{18-x}(SBB)_x$ with higher polarity was eluted sequentially by decreasing the polarity of the mobile phase using a gradient program (Fig. 14A). It is assumed that the difference in the adsorption ability to the stationary phase was also involved in this separation in addition to the difference in the partition coefficient. Niihori *et al.* demonstrated that such a method is applicable to the separation of various $Au_{24}Pd(SR_1)_{m-x}(SR_2)_x$ clusters with two types of SRs (Fig. 14B).[172] In later studies, Niihori *et al.* also succeeded in further improving the resolution, thereby enabling the separation of $Au_{24}Pd(SC_2H_4Ph)_{18-x}(SC_{12}H_{25})_x$ ($x = 1, 2$) depending on the coordination isomers (Fig. 14C).[173] Such separation revealed a preferred site for ligand exchange.[173]

5.1.4. Separation of alloy clusters depending on the chemical composition of the metal core. Replacing Au atoms in $Au_n(SR)_m$ clusters with another metal is expected to produce new electronic structures, physical/chemical properties, and functions different from those of the monometallic $Au_n(SR)_m$ clusters. Therefore, research on alloy clusters has recently become a hot topic.[23,53,162–165,172,174–213] To deeply understand the correlation between the structure and physical/chemical properties in such an alloy cluster, it is necessary to control the chemical composition of the alloy cluster. Synthesis methods with atomic precision have already been established for several alloy clusters. However, many alloy clusters cannot be synthesized yet with atomic precision. The representative clusters are 25-atom and 38-atom clusters composed of Au and Ag ($Au_{25-x}Ag_x(SR)_{18}$ and $Au_{38-x}Ag_x(SR)_{24}$).[163,164,210,214] Using RP partition chromatography, it is also possible to separate these mixtures depending on the chemical composition of the metal core.

Niihori *et al.* prepared a mixture of $Au_{25-x}Ag_x(SC_4H_9)_{18}$ ($x = 1–4$) (SC_4H_9 = butanethiolate) and separated it using RP par-
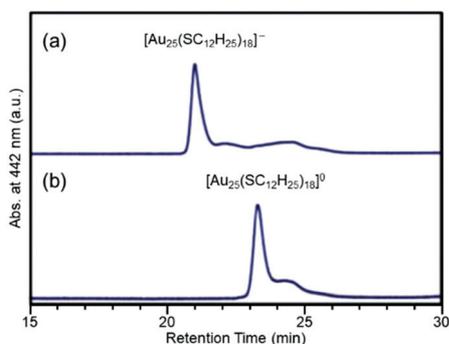
Fig. 13 RP partition chromatograms of (a) $[Au_{25}(SC_{12}H_{25})_{18}]^-$ and (b) $[Au_{25}(SC_{12}H_{25})_{18}]^0$. Reproduced with permission from ref. 162. Copyright 2010 The Royal Society of Chemistry.
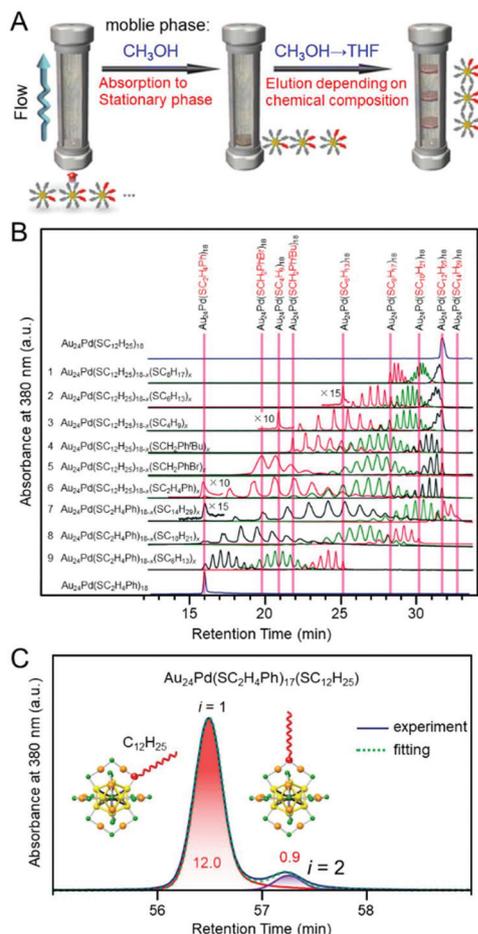
Fig. 14 HPLC separation of $Au_{24}Pd(SR_1)_{18-x}(SR_2)_x$ clusters depending on the ligand combination. (A) Schematic illustration of separation method.[171] (B) Chromatogram of $Au_{24}Pd(SR_1)_{18-x}(SR_2)_x$ clusters.[172] (C) Expanded chromatogram of $Au_{24}Pd (SC_2H_4Ph)_{17}(SC_{12}H_{25})$, showing the separation of the coordination isomers.[173] Reproduced with permission from ref. 171, 172 and 173. Copyright 2013 American Chemical Society, Copyright 2014 The Royal Society of Chemistry, and Copyright 2015 American Chemical Society.

Fig. 15 (A) Separation of $[Au_{25-x}Ag_x(SC_4H_9)_{18}]^0$. (a) Negative-ion ESI mass spectrum and (b) UV chromatogram and the fitting result of a cluster mixture. (c) Negative-ion ESI mass spectra and isotope patterns for peaks i–v in (b). (d) Time-dependent mass spectrum and (e) extracted-ion (EI) chromatogram. In (e), the total ion (TI) chromatogram overall reproduces the UV chromatogram (b). (B) Optical absorption spectra of i ($[Au_{25}(SC_4H_9)_{18}]^0$), ii ($[Au_{24}Ag(SC_4H_9)_{18}]^0$), iii ($[Au_{23}Ag_2(SC_4H_9)_{18}]^0$), v ($[Au_{22}Ag_3(SC_4H_9)_{18}]^0$), and iv' ($[Au_{21}Ag_4(SC_4H_9)_{18}]^0$; the mass spectrum is shown in the original paper. In the red, blue, and green regions, the clear peak splitting is caused by Ag substitution. Reproduced with permission from ref. 212. Copyright 2018 American Chemical Society.

tition chromatography. In this study, they used a column with a core–shell-type stationary phase. As a result, $Au_{25-x}Ag_x(SC_4H_9)_{18}$ ($x = 1–4$) was separated at high resolution (Fig. 15A).[212] The optical absorption spectrum of the separated $Au_{25-x}Ag_x(SC_4H_9)_{18}$ revealed the correlation between the chemical composition and electronic structure in $Au_{25-x}Ag_x(SC_4H_9)_{18}$ ($x = 1–4$) with atomic accuracy (Fig. 15B). This method also enabled the separation of structural isomers in $Au_{25-x}Ag_x(SC_4H_9)_{18}$ ($x = 2,3$) (Fig. 15A).[212] The researchers recorded time-dependent mass spectra using LC/MS for $Au_{25-x}Ag_x(SC_4H_9)_{18}$ ($x = 1–4$). They revealed that $Au_{25-x}Ag_x(SC_4H_9)_{18}$ ($x = 2,3$) has different structural isomer distributions depending on the synthesis method and that the isomer distributions vary in solution. Similar separation and evaluation were also performed by Niihori *et al.* for $Au_{38-x}Ag_x(SC_4H_9)_{24}$ ($x = 1–4$).[213]

5.2. Ion-pair chromatography

As described in section 4, PAGE has been mainly used for the separation of hydrophilic clusters. However, if RP partition chromatography can be used for the separation of hydrophilic clusters, it becomes possible to determine the chemical composition of the separated clusters using LC/MS. The separation of such hydrophilic clusters by RP partition chromatography can be achieved by changing the hydrophilic surface of the cluster to a hydrophobic surface with an ion-pair reagent (Fig. 16A).[215] There have been several reports on the separation
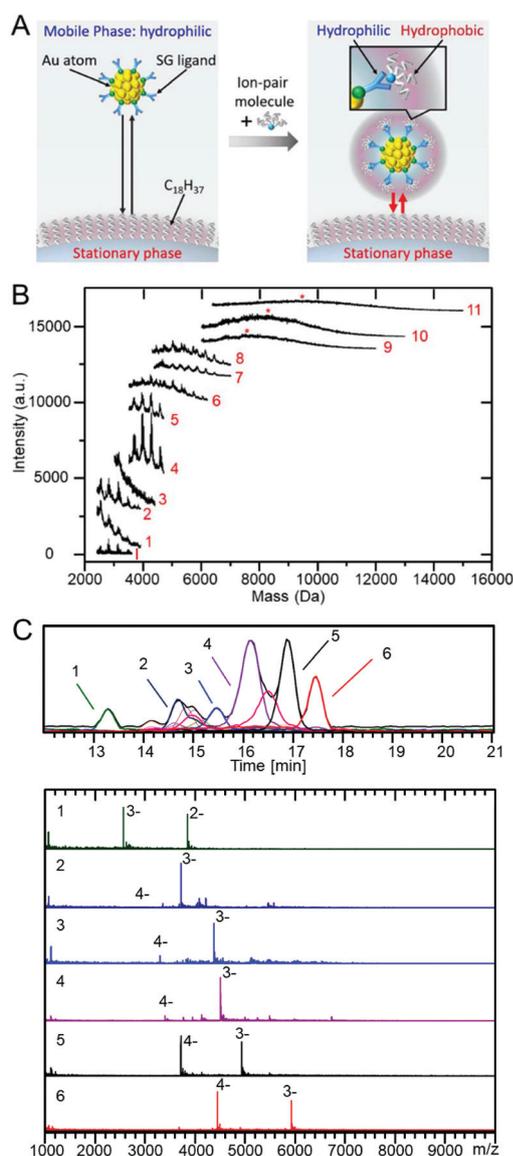
Fig. 16 (A) Diagram showing the basic concept of reverse phase ion-pair chromatography in the separation of hydrophilic $Au_n(SR)_m$ clusters.[215] (B) MALDI mass spectra of each fraction (1–11) separated by ion-pair chromatography.[217] (C) ESI-coupled LC/MS analysis of $Au_n(m$-$MBA)_m$ clusters. The top frame shows the chromatograms and an EI chromatogram for each identified component.[221] Reproduced with permission from ref. 215, 217 and 221. Copyright 2017 American Chemical Society, Copyright 2009 American Chemical Society, and Copyright 2019 MDPI.

of hydrophilic clusters depending on the core size using such ion-pair chromatography.

The first report was on the separation of $Au_n(NALC)_m$ and $Au_n(S(PG))_m$ clusters (NALC = N-acetyl-L-cysteine) by Murray et al. In this study, they used a C18 column for the stationary phase and tetrabutylammonium fluoride $((C_4H_9)_4N^+F^-)$ for the ion-pair reagent.[216] $Au_n(NALC)_m$ and $Au_n(S(PG))_m$ clusters were separated depending on the core size because $(C_4H_9)_4N^+$ ions formed ion pairs with hydrophilic clusters, and therefore, the cluster surface caused a hydrophobic interaction with the stationary phase. Later,

Choi et al. attempted to separate $Au_n(NALC)_m$ clusters under similar experimental conditions. In the study by Murray et al., the separated $Au_n(NALC)_m$ clusters were characterized by optical absorption spectroscopy.[216] However, Choi et al. separated each fraction and obtained their MALDI mass spectra (Fig. 16B). They confirmed that the $Au_n(NALC)_m$ clusters could be separated depending on the chemical composition using this method.[217] They also attempted to separate $Au_n(NALC)_m$ clusters using an ultra HPLC (UHPLC) instrument. The results indicated that the separation could be performed in approximately 10% of the retention time with sharper peaks appearing in the chromatogram compared with the results obtained using the normal HPLC apparatus.[218] Dong and Choi et al. conducted similar experiments on $Pd_n(NALC)_m$ clusters and succeeded in separating them depending on the chemical composition.[219] Niihori et al. performed the separation of $Au_n(SG)_m$ clusters including the most commonly used hydrophilic ligand, SG, using ion-pair chromatography and succeeded in achieving higher-resolution separation than PAGE separation.[215]

In these studies, ion-pair chromatography was used for the separation; however, the chemical composition of the separated clusters was not determined by LC/MS. Because $(C_4H_9)_4N^+$ easily forms an ion pair with the dissociable functional group of the ligand and easily interacts with the stationary phase, a relatively high-resolution separation could be achieved when $(C_4H_9)_4N^+$ is used as the ion-pair reagent. However, $(C_4H_9)_4N^+$ is non-volatile and cannot be used in LC/MS because the salt precipitates during the ionization process. Whetten et al. overcame these challenges by using volatile triethylamine as the ion-pair reagent and succeeded in both the separation and determination of the chemical composition of the separated species by LC/MS for $Au_n(p$-$MBA)_m$ (n = 5–102, m = 5–44) and $Au_n(m$-$MBA)_m$ clusters (m-MBA = m-mercaptobenzoic acid; n = 48–67, m = 26–30; Fig. 16C).[220,221] Whetten et al. also succeeded in identifying $Au_{146}(p$-$MBA)_{57}$ and $[Ag_{29}(LA)_{12}]^{3-}$ (LA = (R)-α lipoic acid) clusters and performing structural analysis of $[Ag_{29}(LA)_{12}]^{3-}$.[222,223]

5.3. Hydrophilic interaction liquid chromatography

In this way, by using an ion-pair reagent, it is possible to separate the hydrophilic clusters depending on the core size using RP partition chromatography. In addition, when a volatile ion-pair reagent is used, the chemical composition of the separated clusters can be determined using an ESI mass spectrometer directly connected with RP partition chromatography. However, if a hydrophilic interaction liquid chromatography (HILIC) column[224] was used for the separation of the hydrophilic clusters, even ion-pair reagents become unnecessary, and the separation and evaluation of hydrophilic clusters would be facilitated.

Niihori et al. attempted the separation and evaluation of $Au_n(SG)_m$ and $Au_{n-x}M_x(SG)_m$ alloy clusters (M = Ag, Cu or Pd) by LC/MS using an HILIC column (Fig. 17A). They used two columns (a ZIC-cHILIC and Amido-80 column; Fig. 11B). The $Au_n(SG)_m$ clusters were separated with high resolution.[211] In this study, they detected the $Au_n(SG)_m$ clusters that had never been reported (Fig. 17B). All the synthesized clusters were introduced into the mass spectrometer, unlike the case using
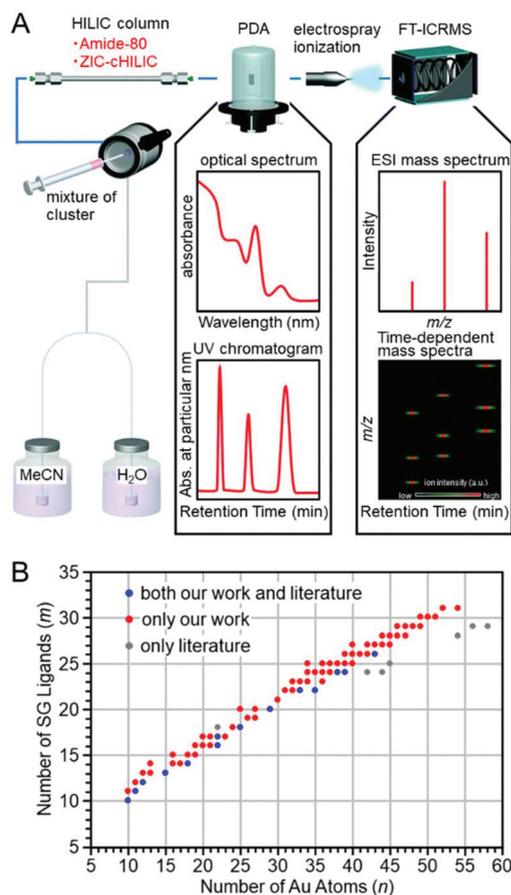
Fig. 17 (A) Schematic illustration of the LC/MS system used in the work of ref. 211. PDA: Photodiode array, FT-ICRMS: Fourier transform-ion cyclotron resonance mass spectrometry. (B) Comparison of chemical compositions of $Au_n(SG)_m$ clusters determined by ESI mass spectrometry. Reproduced with permission from ref. 211. Copyright 2018 The Royal Society of Chemistry.

PAGE (Fig. 17A). Thus, small species that have almost never been observed before were also detected in addition to the previously reported stable species. The use of the HILIC column also enabled the separation of $Au_{n-x}M_x(SG)_m$ alloy clusters depending on the number of constituent atoms. The chemical composition evaluation by LC/MS resulted in the discovery of new $Au_{n-x}Pd_x(SG)_m$ clusters, such as $Au_{14}Pd(SG)_{13}$, $Au_{24}Pd(SG)_{18}$, and $Au_{28}Pd(SG)_{20}$, which had not been reported until then. Stamplecoskie et al. also separated $Ag_n(SG)_m$ clusters using an amide column and revealed the size dependence of the optical properties of $Ag_n(SG)_m$ clusters[225] (although the technique is not described as HILIC in the original paper, it is speculated that each $Ag_n(SG)_m$ cluster was separated in HILIC mode from the experimental conditions).

5.4. Size exclusion chromatography

In the RP partition chromatography and the HILIC described above, a chemical interaction (partitioning and/or adsorption)

occurs between the stationary phase and clusters, and accordingly, the difference in the mobility of each cluster results in the separation of the clusters. However, in size exclusion chromatography (SEC), each cluster is separated by physical size. Therefore, when separating the clusters using the size exclusion mode, a stationary phase that does not interact with the clusters must be selected. SEC is divided into gel permeation chromatography (GPC) and gel filtration chromatography (GFC). In GPC, the mobile phase is an organic solvent, and in GFC, the mobile phase is an aqueous solvent. In these separations, $Au_n(SR)_m$ clusters elute from the column in the order from largest to smallest.

5.4.1. Gel permeation chromatography. It is reasonable to first consider using SEC for the separation of $Au_n(SR)_m$ clusters depending on the core size. Wilcoxon et al. attempted to separate $Au_n(SR)_m$ clusters using GPC in 2000.[226] In this study, porous organics were used as the stationary phase (Fig. 11C). When this experiment was conducted, it was not yet possible to determine the chemical composition of $Au_n(SR)_m$ clusters with atomic precision. Therefore, in their earlier work, they synthesized $Au_n(SC_lH_{2l+1})_m$ clusters with similar metal core sizes (~2 nm) using several SC_lH_{2l+1} with different alkyl chain lengths ($l = 6–18$). Then, the thickness of the ligand layer in each $Au_n(SC_lH_{2l+1})_m$ cluster ($l = 6–18$) was studied by comparing their retention times. Regarding the thickness of the ligand layer, Tsukuda et al. also later studied $Pd_n(SC_lH_{2l+1})_m$ clusters ($l = 10, 12, 14, 16,$ or 18).[227]

Wilcoxon et al. then performed the size separation of $Au_n(SC_lH_{2l+1})_m$ and $Ag_n(SC_{12}H_{25})_m$ clusters with a metal core size of 1.3–8.0 nm. They obtained knowledge on the correlation between the particle size and electronic structure from their findings.[228,229] Tsukuda et al. succeeded in separating $Au_n(SC_{18}H_{37})_m$ clusters with higher resolution by recycling (Fig. 18A),[230] and successfully isolated $Au_n(SC_lH_{2l+1})_m$ clusters ($l = 12, 18$) having Au_{55} as the metal core with high purity.[231] In a later study, Jin et al. revealed that this cluster has the chemical composition of $Au_{55}(SR)_{31}$ using ESI-MS (Fig. 18B).[232] Jin et al. also succeeded in separating $Au_{38}(SC_2H_4Ph)_{24}$ and $Au_{40}(SC_2H_4Ph)_{24}$, whose chemical compositions are very similar, using GPC.[233]

GPC is also utilized for tracking reactions. Negishi et al. traced the growth of $Ag_n(SBB)_m$ clusters using GPC. The clusters were observed to settle in a stable cluster at 96 h under their reaction conditions (Fig. 18C).[234] Jin et al. and Zhu et al. also used GPC to track several reactions and discovered a method to size-selectively synthesize $Au_n(SR)_m$ clusters, such as $Au_{19}(SC_2H_4Ph)_{13}$, $Au_{20}(SC_2H_4Ph)_{16}$, and $Au_{24}(SC_2H_4Ph)_{20}$, with atomic precision.[235,236]

5.4.2. Gel filtration chromatography. For the separation of hydrophilic clusters, there have only been a few reports on the separation by GFC because PAGE is frequently used for these clusters. Thus, the purpose of GFC separation is limited to cluster purification (Fig. 18D).[237] Inouye et al. used GFC to purify mercaptoacetic acid (MAA)-protected Pt clusters $(Pt_n(MAA)_m)$. In this experiment, they used a stationary phase consisting of porous silica (Fig. 11D). They succeeded in isolat-
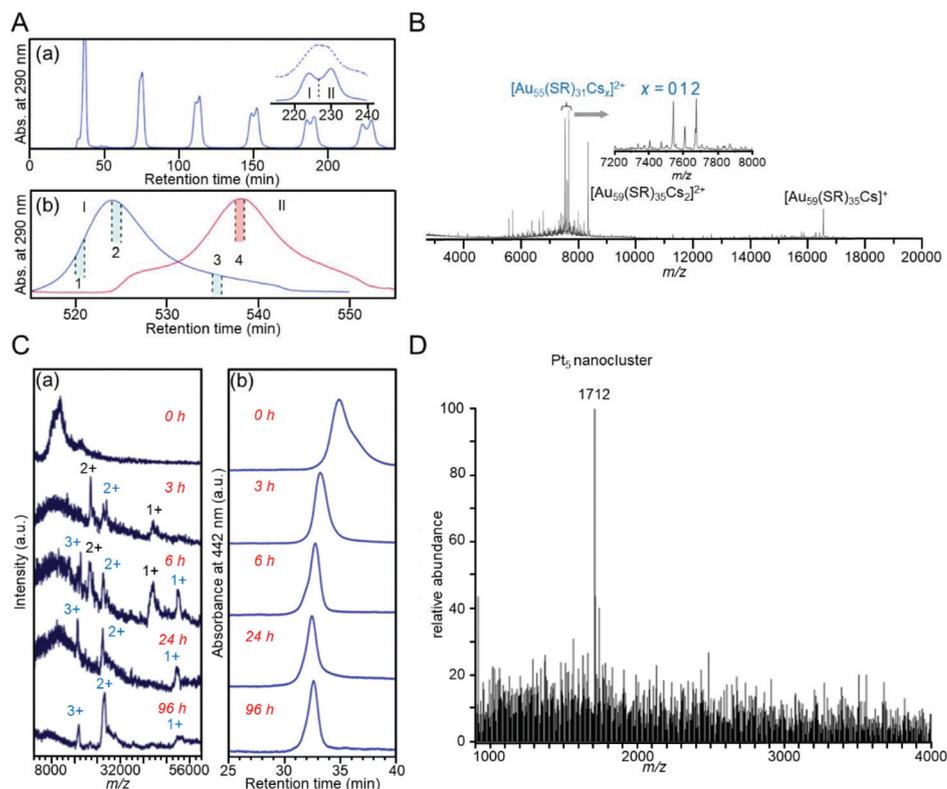
Fig. 18 Examples of SEC separations. (A) (a) Chromatogram of recycling GPC of the $Au_n(SC_{18}H_{25})_m$ clusters reported by the Tsukuda group.[230] The dotted curve in the inset is the data for the sample without etching treatment. (b) Recycling chromatograms of two fractions I and II. Fraction 2 includes the Au_{55} cluster with high purity. (B) ESI mass spectrum of $[Au_{55}(SR)_{31}Cs_x]^{2+}$ observed by the Jin group.[232] (C) (a) Positive-ion ESI mass spectra and (b) GPC chromatograms of $Ag_n(SBB)_m$ clusters as a function of incubation time (incubation by BBSH).[234] (D) ESI mass spectrum of the Pt_5 nanocluster obtained by GFC purification.[237] Reproduced with permission from ref. 230, 232, 234 and 237. Copyright 2006 American Chemical Society, Copyright 2011 The Royal Society of Chemistry, Copyright 2011 The Royal Society of Chemistry, and Copyright 2011 Wiley-VCH.

ing $Pt_5(MAA)_8$, which emits blue light, and $Pt_8(C_2H_2O_2S)_8$, which emits green light, with high purity using GFC.[238]

5.5. Chiral chromatography

In chiral chromatography, a compound is separated into optical isomers by utilizing the difference in interaction between the compound and a stationary phase with chirality. The stationary phase is composed of silica gel chemically modified with a chiral compound, such as cellulose (Fig. 11E). A "three-point bond model" has been proposed for the separation mechanism of the optical isomers.[239] According to this mechanism, a compound and a chiral stationary phase form a diastereomeric aggregate because of interaction at three binding sites. Because the binding energy of such an aggregate differs depending on the optical isomer (Fig. 11E), a difference in the retention time of each optical isomer is observed. Interactions forming aggregates include hydrogen-bond formation, charge-transfer complex formation, ion-pair formation, coordination bonding to metals, and dipole–dipole interaction. In the actual separation, these interactions contribute singly or in combination.

Kornberg *et al.* determined the geometrical structure of the $Au_n(SR)_m$ cluster for the first time in 2007, revealing that the $Au_n(SR)_m$ cluster consisted of a Au core covered with multiple Au(I)–SR staples and that $Au_{102}(p\text{-MBA})_{44}$ has optical isomers.[240] Since then, many $Au_n(SR)_m$ clusters have been revealed to have optical isomers by SC-XRD analysis.[61,241–243]

Bürgi *et al.* succeeded for the first time in separating $Au_{38}(SC_2H_4Ph)_{24}$ (Fig. 19A) into chiral isomers using chiral chromatography in 2010 (Fig. 19B).[244] In this study, a stationary phase in which cellulose was chemically modified on the silica surface was used. The separation resulted in obtaining much information on the physical/chemical properties of the chiral $Au_n(SR)_m$ clusters, which were previously unknown. For example, for the chemical properties, it was revealed that when one of the optical isomers of $Au_{38}(SC_2H_4Ph)_{24}$ was left in a solvent at 80 °C, racemization proceeded and the enantiomeric excess became 27% in 15 min.[245] The researchers performed the same separation and reaction tracking for $Au_{40}(SC_2H_4Ph)_{24}$ and observed that $Au_{40}(SC_2H_4Ph)_{24}$ does not racemize unless it is left in solution at a higher temperature.[246] The researchers also revealed that the two optical isomers had different reaction rates in the ligand exchange reaction with 1,1′-binaphthyl-2,2′-dithiol (*R*-BINAS), which has optical iso-
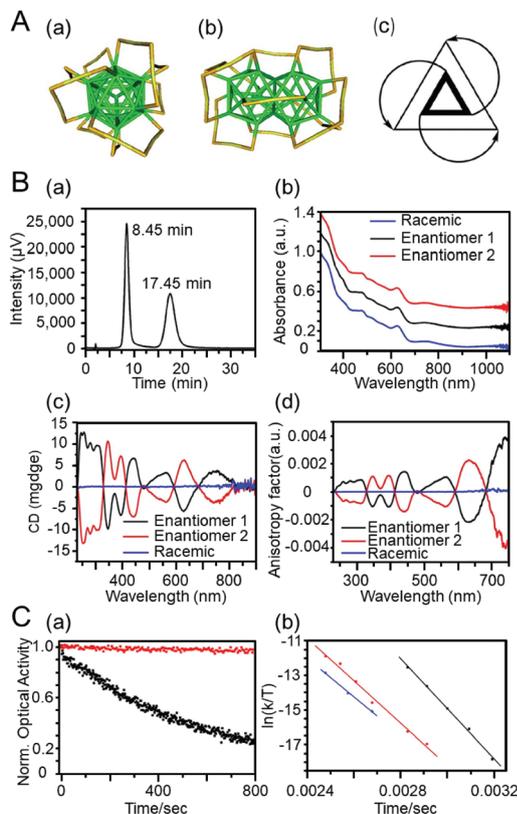
Fig. 19 (A) Crystal structure of the left-handed enantiomer of $Au_{38}(SC_2H_4Ph)_{24}$. For clarity, the $-C_2H_4Ph$ units were removed; yellow, gold adatoms; green, core atoms (Au); orange, sulfur. (a) Top view and (b) side view of the cluster; (c) schematic representation highlighting the handedness of the cluster. (B) HPLC separation of rac-$Au_{38}(SC_2H_4Ph)_{24}$. (a) HPLC chromatogram of the enantioseparation of rac-$Au_{38}(SC_2H_4Ph)_{24}$. The peak at 8.45 min corresponds to enantiomer 1; the second peak at 17.45 min corresponds to enantiomer 2. (b) Optical absorbance spectra of enantiomers 1 (black) and 2 (red) and of the race-mate (blue). (c) CD spectra of isolated enantiomers 1 (black) and 2 (red) and of rac-$Au_{38}(SC_2H_4Ph)_{24}$ (blue) before separation and (d) corresponding anisotropy factors of enantiomers 1 and 2 and of the race-mate.[244] (C) (a) CD response of $Au_{38}(SC_2H_4Ph)_{24}$ (black) and A-$Au_{38}(SC_2H_4Ph)_{22}(R$-BINAS$)_1$ (red) during heating at 80 °C. (b) Eyring plot showing the temperature dependency of the rate constants of the inversion for $Au_{38}(SC_2H_4Ph)_{24}$ (black), A-$Au_{38}(SC_2H_4Ph)_{22}(R$-BINAS$)_1$ (red), and C-$Au_{38}(SC_2H_4Ph)_{22}(R$-BINAS$)_1$ (blue).[248] Reproduced with permission from ref. 244 and 248. Copyright 2012 Nature Publishing Group and Copyright 2013 American Chemical Society.

merism.[247] It was also clarified that introducing R-BINAS into the ligand layer by ligand exchange improves the stability of the cluster and can suppress the racemization of the optical isomer (Fig. 19C).[248] Soai and Negishi et al. studied the asymmetric autocatalytic reaction (Soai reaction[249]) in which a chiral compound asymmetrically synthesizes itself and self-proliferates using each optical isomer of $Au_{38}(SC_2H_4Ph)_{24}$.[250] This study revealed that each optical isomer of $Au_{38}(SC_2H_4Ph)_{24}$ can be used as an asymmetric catalyst.

Chiral chromatography has also been used for the optical separation of other $Au_n(SR)_m$ and related clusters.[251–261] The use of such chiral chromatography is expected to provide a

deeper understanding of the asymmetric catalytic activity and circularly polarized light emission[262] of each optical isomer in the future.

6. TLC separation

TLC uses an inexpensive and simple device different from that used for HPLC. Furthermore, in TLC, the separation can be visually confirmed similarly to PAGE. The use of preparative thin-layer chromatography (PTLC) using a thicker silica gel than that used in TLC makes it possible to isolate each cluster on a relatively large scale. Therefore, TLC is often used to confirm the purity of a product. When Wu and Jin et al. elucidated the geometrical structure of $Au_{144}(SR)_{60}$ by SC-XRD, PTLC was used to increase its purity.[263] For a mixture of $Au_n(SR)_m$ and related clusters composed of clusters with great difference in size and charge state, this method can be used for the separation of clusters depending on the size and charge state.

Pradeep et al. succeeded in clearly separating $Au_{25}(SC_2H_4Ph)_{18}$ and $Au_{144}(SC_2H_4Ph)_{60}$ contained in the product using TLC in 2014.[264] They also succeeded in separating $Au_{25}(SC_2H_4Ph)_{18}$ and $Au_{25}(SC_4H_9)_{18}$ with different ligands, $Au_{25}(Calix)_x(SC_4H_9)_y$ (Calix = tetrathiolated calix[4]arene (25,26,27,28-tetrakis (4-mercapto-n-butoxy)calix[4]arene); Fig. 20A) with different ligand combi-
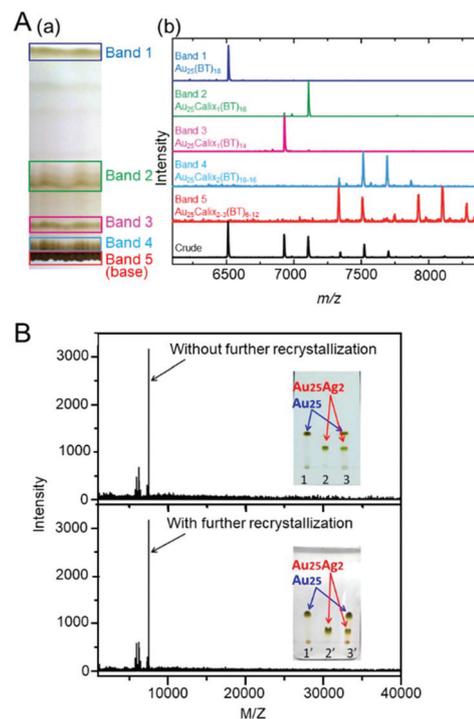
Fig. 20 (A) (a) Photograph of the TLC plate used for cluster separation. (b) MALDI-MS data for the $Au_{25}Calix_{0-3}BT_{6-18}$ crude product before TLC (black trace) and bands 1–5 separated by TLC.[264] (B) Inset: TLC chromatogram of Au_{25} (1 and 1'), $Au_{25}Ag_2$ (2 and 2') and of the mixture of Au_{25} and $Au_{25}Ag_2$ (3 and 3').[265] Reproduced with permission from ref. 264 and 265. Copyright 2014 American Chemical Society and Copyright 2015 American Chemical Society.

nations, and $[Au_{25}(SC_2H_4Ph)_{18}]^0$ and $[Au_{25}(SC_2H_4Ph)_{18}]^-$ with different charge states using TLC. Wu *et al.* clearly separated $Au_{25}(SC_2H_4Ph)_{18}$ and $Au_{25}Ag_2(SC_2H_4Ph)_{18}$ using TLC (Fig. 20B).[265] Jin *et al.* succeeded in separating the structural isomers (T- and Q-isomers) of $Au_{38}(SC_2H_4Ph)_{24}$ using TLC.[266]

TLC is also frequently used in identifying the optimal reaction conditions because the distribution of the product can be visually confirmed. Wu *et al.* reacted $[Au_{25}(SC_2H_4Ph)_{18}]^-$ with Ag(I) ions and evaluated the distribution of the product. The analyses revealed that the anti-galvanic reaction occurring between $[Au_{25}(SC_2H_4Ph)_{18}]^-$ with Ag(I) ions varied depending on the type and concentration of Ag(I) ions.[267] Wu *et al.* also used PTLC to monitor the size conversion from $Au_{44}(TBBT)_{28}$ (TBBT = 4-*tert*-butylbenzenethiolate) to $Au_{36}(TBBT)_{24}$. As a result, they succeeded in finding effective reaction conditions for such exchange reactions.[268]

7. Summary and outlook

This review summarized previous research on the high-resolution separation of $Au_n(SR)_m$ and related clusters by focusing on PAGE, HPLC, and TLC. From this summary, the following characteristics of each separation method were revealed.

PAGE:

Main target: Hydrophilic clusters

Advantages: (i) Inexpensive and simple, (ii) possible to separate clusters containing 40 or less atoms with atomic precision, and (iii) possible to confirm separation visibly by the naked eye

Main applications: (i) Isolation, (ii) reaction tracking, (iii) search for/identification of photoluminescent clusters, (iv) structural analysis, and (v) washing/purification

HPLC:

Main target: Both hydrophobic and hydrophilic clusters

Advantages: (i) High resolution, (ii) high repeatability, (iii) variety of separation modes, (iv) chiral separation, (v) possible to connect with an ESI mass spectrometer, (vi) possible to analyse minor species, and (vii) short separation time (UHPLC)

Main applications: (i) Isolation (but small amount), (ii) reaction tracking, (iii) structural analysis, (iv) chiral separation, and (v) washing/purification

TLC:

Main target: Hydrophobic clusters

Advantages: (i) Inexpensive and simple, (ii) possible to confirm separation visibly by the naked eye

Main applications: (i) Isolation, (ii) reaction tracking, (iii) structural analysis, and (iv) washing/purification

Because the precise synthesis techniques of $Au_n(SR)_m$ and related clusters have progressed rapidly in the last 20 years, many studies on their separation have been reported. We hope that this review will provide guidelines to understand the characteristics of each separation method and enable the selection of an appropriate separation method for the target experiment.

In addition, it is hoped that the established techniques will be used more widely in the future for the separation of metal clusters. The chemical properties of $Au_n(SR)_m$ and related clusters have still not been clarified completely. For example, although it has been revealed that many $Au_n(SR)_m$ and related clusters have a chiral structure, the asymmetric catalytic activity and circularly polarized luminescence of each optical isomer have not yet been revealed. It is expected that these physical/chemical properties can be elucidated by studying each optical isomer separated by chiral chromatography. In addition, metal exchange between $Au_{n-x}M_x(SR)_m$ clusters has been shown to occur in solution.[20] However, there are still many unclear points about the mechanism of the metal exchange reaction. A deep understanding of this mechanism could be obtained if the reaction proceeded using $Au_{n-x}Ag_x(SR)_m$ clusters isolated with atomic precision[211,212] and the reaction process was tracked using LC/MS. In future studies, the effective use of established separation techniques is expected to provide a deep understanding of the functions and properties of $Au_n(SR)_m$ and related clusters.

Furthermore, there are some helpful separation/analysis techniques that should be actively incorporated in future research on metal clusters. For example, MS/MS in LC/MS is useful not only for determining the chemical composition of a product but also for analysing the structure of the product.[269] An introduction of two-dimensional HPLC is also interesting for analysis.[270] If such a method is introduced, comprehensive two-dimensional separation could be realised using two different separation modes. For instance, an optical isomer generated based on the position of an exchange ligand is expected to be isolated by this method.

As introduced in this review, separation/analysis techniques for metal clusters have been developing with the improvement of separation and analysis equipment. HPLC columns and mass spectrometers are still being improved day after day. We hope that the separation and analysis techniques for metal clusters will continue to evolve in the future with researchers being conscious of the latest techniques available for each device and continuing to actively incorporate such techniques into research on metal clusters.

Author contributions

Y. Negishi constructed the structure of this review. T. Kawawaki wrote sections 1 and 7. K. Hamada wrote sections 2 and 3. S. Hashimoto and A. Ebina wrote sections 4–6. Y. Negishi and S. Hossain revised the entire draft before submission, and all the authors have approved the final version of the manuscript.

Conflicts of interest

There are no conflicts to declare.

Notes and references

1 K. J. Taylor, C. L. Pettiette-Hall, O. Cheshnovsky and R. E. Smalley, *J. Chem. Phys.*, 1992, **96**, 3319–3329.

2 K. Miyajima, N. Fukushima, H. Himeno, A. Yamada and F. Mafuné, *J. Phys. Chem. A*, 2009, **113**, 13448–13450.

3 A. Nakajima, K. Hoshino, K. Watanabe, Y. Konishi, T. Kurikawa, S. Iwata and K. Kaya, *Chem. Phys. Lett.*, 1994, **222**, 353–357.

4 Y. Negishi, Y. Nakamura, A. Nakajima and K. Kaya, *J. Chem. Phys.*, 2001, **115**, 3657–3663.

5 K. Tono, A. Terasaki, T. Ohta and T. Kondow, *Chem. Phys. Lett.*, 2007, **449**, 276–281.

6 T. Watanabe and T. Tsukuda, *J. Phys. Chem. C*, 2013, **117**, 6664–6668.

7 C. E. Briant, B. R. C. Theobald, J. W. White, L. K. Bell, D. M. P. Mingos and A. J. Welch, *J. Chem. Soc., Chem. Commun.*, 1981, 201–202.

8 G. Schmid, R. Pfeil, R. Boese, F. Bandermann, S. Meyer, G. H. M. Calis and J. W. A. van der Veldend, *Chem. Ber.*, 1981, **114**, 3634–3642.

9 S. S. Kurasov, N. K. Eremenko, Y. L. Slovokhotov and Y. T. Struchkov, *J. Organomet. Chem.*, 1989, **361**, 405–408.

10 M. McPartlin, R. Mason and L. Malatesta, *J. Chem. Soc. D*, 1969, 334.

11 E. G. Mednikov and L. F. Dahl, *Philos. Trans. R. Soc., A*, 2010, **368**, 1301–1332.

12 G. Schmid, *Chem. Rev.*, 1992, **92**, 1709–1727.

13 M. Schulz-Dobrick and M. Jansen, *Z. Anorg. Allg. Chem.*, 2007, **633**, 2326–2331.

14 B. K. Teo, X. Shi and H. Zhang, *J. Am. Chem. Soc.*, 1992, **114**, 2743–2745.

15 F. A. Vollenbroek, J. J. Bour and J. W. A. van der Veden, *Recl. Trav. Chim. Pays-Bas*, 1980, **99**, 137–141.

16 M. Agrachev, M. Ruzzi, A. Venzo and F. Maran, *Acc. Chem. Res.*, 2019, **52**, 44–52.

17 C. M. Aikens, *Acc. Chem. Res.*, 2018, **51**, 3065–3073.

18 B. Bhattarai, Y. Zaker, A. Atnagulov, B. Yoon, U. Landman and T. P. Bigioni, *Acc. Chem. Res.*, 2018, **51**, 3104–3113.

19 M. Brust, M. Walker, D. Bethell, D. J. Schiffrin and R. Whyman, *J. Chem. Soc., Chem. Commun.*, 1994, 801–802.

20 I. Chakraborty and T. Pradeep, *Chem. Rev.*, 2017, **117**, 8208–8271.

21 Z. Gan, N. Xia and Z. Wu, *Acc. Chem. Res.*, 2018, **51**, 2774–2783.

22 A. Ghosh, O. F. Mohammed and O. M. Bakr, *Acc. Chem. Res.*, 2018, **51**, 3094–3103.

23 S. Hossain, Y. Niihori, L. V. Nair, B. Kumar, W. Kurashige and Y. Negishi, *Acc. Chem. Res.*, 2018, **51**, 3114–3124.

24 R. Jin, C. Zeng, M. Zhou and Y. Chen, *Chem. Rev.*, 2016, **116**, 10346–10413.

25 K. Kwak and D. Lee, *Acc. Chem. Res.*, 2019, **52**, 12–22.

26 B. Nieto-Ortega and T. Bürgi, *Acc. Chem. Res.*, 2018, **51**, 2811–2819.

27 Y. Pei, P. Wang, Z. Ma and L. Xiong, *Acc. Chem. Res.*, 2019, **52**, 23–33.

28 H. Qian, M. Zhu, Z. Wu and R. Jin, *Acc. Chem. Res.*, 2012, **45**, 1470–1479.

29 N. A. Sakthivel and A. Dass, *Acc. Chem. Res.*, 2018, **51**, 1774–1783.

30 Q. Tang, G. Hu, V. Fung and D.-e. Jiang, *Acc. Chem. Res.*, 2018, **51**, 2793–2802.

31 R. L. Whetten, H.-C. Weissker, J. J. Pelayo, S. M. Mullins, X. López-Lozano and I. L. Garzón, *Acc. Chem. Res.*, 2019, **52**, 34–43.

32 J. Yan, B. K. Teo and N. Zheng, *Acc. Chem. Res.*, 2018, **51**, 3084–3093.

33 Q. Yao, T. Chen, X. Yuan and J. Xie, *Acc. Chem. Res.*, 2018, **51**, 1338–1348.

34 R. L. Whetten, J. T. Khoury, M. M. Alvarez, S. Murthy, I. Vezmar, Z. L. Wang, P. W. Stephens, C. L. Cleveland, W. D. Luedtke and U. Landman, *Adv. Mater.*, 1996, **8**, 428–433.

35 T. G. Schaaff, M. N. Shafigullin, J. T. Khoury, I. Vezmar, R. L. Whetten, W. G. Cullen, P. N. First, C. Gutiérrez-Wing, J. Ascensio and M. J. Jose-Yacamán, *J. Phys. Chem. B*, 1997, **101**, 7885–7891.

36 R. L. Donkers, D. Lee and R. W. Murray, *Langmuir*, 2004, **20**, 1945–1952.

37 R. S. Ingram, M. J. Hostetler, R. W. Murray, T. G. Schaaff, J. T. Khoury, R. L. Whetten, T. P. Bigioni, D. K. Guthrie and P. N. First, *J. Am. Chem. Soc.*, 1997, **119**, 9279–9280.

38 T. G. Schaaff, M. N. Shafigullin, J. T. Khoury, I. Vezmar and R. L. Whetten, *J. Phys. Chem. B*, 2001, **105**, 8785–8796.

39 Y. Shichibu, Y. Negishi, H. Tsunoyama, M. Kanehara, T. Teranishi and T. Tsukuda, *Small*, 2007, **3**, 835–839.

40 A. Desireddy, S. Kumar, J. Guo, M. D. Bolan, W. P. Griffith and T. P. Bigioni, *Nanoscale*, 2013, **5**, 2036–2044.

41 Y. Negishi, K. Nobusada and T. Tsukuda, *J. Am. Chem. Soc.*, 2005, **127**, 5261–5270.

42 Y. Negishi, H. Tsunoyama, M. Suzuki, N. Kawamura, M. M. Matsushita, K. Maruyama, T. Sugawara, T. Yokoyama and T. Tsukuda, *J. Am. Chem. Soc.*, 2006, **128**, 12034–12035.

43 Y. Yu, Z. Luo, D. M. Chevrier, D. T. Leong, P. Zhang, D.-e. Jiang and J. Xie, *J. Am. Chem. Soc.*, 2014, **136**, 1246–1249.

44 Y. Shichibu, Y. Negishi, T. Tsukuda and T. Teranishi, *J. Am. Chem. Soc.*, 2005, **127**, 13464–13465.

45 Y. Du, H. Sheng, D. Astruc and M. Zhu, *Chem. Rev.*, 2020, **120**, 526–622.

46 H. Kawasaki, S. Kumar, G. Li, C. Zeng, D. R. Kauffman, J. Yoshimoto, Y. Iwasaki and R. Jin, *Chem. Mater.*, 2014, **26**, 2777–2788.

47 J. Xie, Y. Zheng and J. Y. Ying, *Chem. Commun.*, 2010, **46**, 961–963.

48 G. Li and R. Jin, *Acc. Chem. Res.*, 2013, **46**, 1749–1758.

49 W. Kurashige, R. Kumazawa, D. Ishii, R. Hayashi, Y. Niihori, S. Hossain, L. V. Nair, T. Takayama, A. Iwase, S. Yamazoe, T. Tsukuda, A. Kudo and Y. Negishi, *J. Phys. Chem. C*, 2018, **122**, 13669–13681.

50 Y. Negishi, Y. Matsuura, R. Tomizawa, W. Kurashige, Y. Niihori, T. Takayama, A. Iwase and A. Kudo, *J. Phys. Chem. C*, 2015, **119**, 11224–11232.

51 Y.-S. Chen, H. Choi and P. V. Kamat, *J. Am. Chem. Soc.*, 2013, **135**, 8822–8825.

52 N. Sakai and T. Tatsuma, *Adv. Mater.*, 2010, **22**, 3185–3188.

53 T. Kawawaki, Y. Negishi and H. Kawasaki, *Nanoscale Adv.*, 2020, **2**, 17–36.

54 Y. Niihori, C. Uchida, W. Kurashige and Y. Negishi, *Phys. Chem. Chem. Phys.*, 2016, **18**, 4251–4265.

55 V. L. Jimenez, D. G. Georganopoulou, R. J. White, A. S. Harper, A. J. Mills, D. Lee and R. W. Murray, *Langmuir*, 2004, **20**, 6864–6870.

56 M. W. Heaven, A. Dass, P. S. White, K. M. Holt and R. W. Murray, *J. Am. Chem. Soc.*, 2008, **130**, 3754–3755.

57 Y. Negishi, N. K. Chaki, Y. Shichibu, R. L. Whetten and T. Tsukuda, *J. Am. Chem. Soc.*, 2007, **129**, 11322–11323.

58 N. K. Chaki, Y. Negishi, H. Tsunoyama, Y. Shichibu and T. Tsukuda, *J. Am. Chem. Soc.*, 2008, **130**, 8608–8610.

59 Y. Song, Y. Li, H. Li, F. Ke, J. Xiang, C. Zhou, P. Li, M. Zhu and R. Jin, *Nat. Commun.*, 2020, **11**, 478.

60 Q. Xu, S. Kumar, S. Jin, H. Qian, M. Zhu and R. Jin, *Small*, 2014, **10**, 1008–1014.

61 H. Qian, W. T. Eckenhoff, Y. Zhu, T. Pintauer and R. Jin, *J. Am. Chem. Soc.*, 2010, **132**, 8280–8281.

62 P. R. Nimmala, B. Yoon, R. L. Whetten, U. Landman and A. Dass, *J. Phys. Chem. A*, 2013, **117**, 504–517.

63 C. Kumara and A. Dass, *Nanoscale*, 2011, **3**, 3064–3067.

64 T. G. Schaaff, G. Knight, M. N. Shafigullin, R. F. Borkman and R. L. Whetten, *J. Phys. Chem. B*, 1998, **102**, 10643–10646.

65 Y. Negishi, Y. Takasugi, S. Sato, H. Yao, K. Kimura and T. Tsukuda, *J. Am. Chem. Soc.*, 2004, **126**, 6518–6519.

66 W. Wang and R. W. Murray, *Langmuir*, 2005, **21**, 7015–7022.

67 T. G. Schaaff and R. L. Whetten, *J. Phys. Chem. B*, 2000, **104**, 2630–2641.

68 K. Kimura, N. Sugimoto, S. Sato, H. Yao, Y. Negishi and T. Tsukuda, *J. Phys. Chem. C*, 2009, **113**, 14076–14082.

69 N. Kothalawala, J. Lee West IV and A. Dass, *Nanoscale*, 2014, **6**, 683–687.

70 K. Ikeda, Y. Kobayashi, Y. Negishi, M. Seto, T. Iwasa, K. Nobusada, T. Tsukuda and N. Kojima, *J. Am. Chem. Soc.*, 2007, **129**, 7230–7231.

71 M. Zhu, C. M. Aikens, F. J. Hollander, G. C. Schatz and R. Jin, *J. Am. Chem. Soc.*, 2008, **130**, 5883–5885.

72 M. Zhu, C. M. Aikens, M. P. Hendrich, R. Gupta, H. Qian, G. C. Schatz and R. Jin, *J. Am. Chem. Soc.*, 2009, **131**, 2490–2492.

73 Y. Negishi, Y. Takasugi, S. Sato, H. Yao, K. Kimura and T. Tsukuda, *J. Phys. Chem. B*, 2006, **110**, 12218–12221.

74 T. Omoda, S. Takano, S. Yamazoe, K. Koyasu, Y. Negishi and T. Tsukuda, *J. Phys. Chem. C*, 2018, **122**, 13199–13204.

75 M. Bieri, C. Gautier and T. Bürgi, *Phys. Chem. Chem. Phys.*, 2007, **9**, 671–685.

76 C. Gautier and T. Bürgi, *J. Am. Chem. Soc.*, 2006, **128**, 11079–11087.

77 H. Yao, T. Fukui and K. Kimura, *J. Phys. Chem. C*, 2008, **112**, 16281–16285.

78 H. Yao, M. Saeki and A. Sasaki, *Langmuir*, 2012, **28**, 3995–4002.

79 S. Kumar, M. D. Bolan and T. P. Bigioni, *J. Am. Chem. Soc.*, 2010, **132**, 13141–13143.

80 J. Guo, S. Kumar, M. Bolan, A. Desireddy, T. P. Bigioni and W. P. Griffith, *Anal. Chem.*, 2012, **84**, 5304–5308.

81 T. Udayabhaskararao, M. S. Bootharaju and T. Pradeep, *Nanoscale*, 2013, **5**, 9404–9411.

82 N. Nishida, H. Yao, T. Ueda, A. Sasaki and K. Kimura, *Chem. Mater.*, 2007, **19**, 2831–2841.

83 M. M. Alvarez, J. Chen, G. Plascencia-Villa, D. M. Black, W. P. Griffith, I. L. Garzón, M. José-Yacamán, B. Demeler and R. L. Whetten, *J. Phys. Chem. B*, 2016, **120**, 6430–6438.

84 S. R. Biltek, S. Mandal, A. Sen, A. C. Reber, A. F. Pedicini and S. N. Khanna, *J. Am. Chem. Soc.*, 2013, **135**, 26–29.

85 N. Cathcart, P. Mistry, C. Makra, B. Pietrobon, N. Coombs, M. Jelokhani-Niaraki and V. Kitaev, *Langmuir*, 2009, **25**, 5840–5846.

86 J. Chen, L. Liu, L. Weng, Y. Lin, L. Liao, C. Wang, J. Yang and Z. Wu, *Sci. Rep.*, 2015, **5**, 16628.

87 L. Dhanalakshmi, T. Udayabhaskararao and T. Pradeep, *Chem. Commun.*, 2012, **48**, 859–861.

88 B. Du, X. Jiang, A. Das, Q. Zhou, M. Yu, R. Jin and J. Zheng, *Nat. Nanotechnol.*, 2017, **12**, 1096–1102.

89 S. Knoppe, M. Vanbel, S. van Cleuvenbergen, L. Vanpraet, T. Bürgi and T. Verbiest, *J. Phys. Chem. C*, 2015, **119**, 6221–6226.

90 G. Li, D.-e. Jiang, S. Kumar, Y. Chen and R. Jin, *ACS Catal.*, 2014, **4**, 2463–2469.

91 Q. Li, Y. Pan, T. Chen, Y. Du, H. Ge, B. Zhang, J. Xie, H. Yu and M. Zhu, *Nanoscale*, 2018, **10**, 10166–10172.

92 S. Maity, D. Bain and A. Patra, *J. Phys. Chem. C*, 2019, **123**, 2506–2515.

93 G. Plascencia-Villa, B. Demeler, R. L. Whetten, W. P. Griffith, M. Alvarez, D. M. Black and M. José-Yacamán, *J. Phys. Chem. C*, 2016, **120**, 8950–8958.

94 T. Udayabhaskararao, B. Nataraju and T. Pradeep, *J. Am. Chem. Soc.*, 2010, **132**, 16304–16307.

95 N. Van Steerteghem, S. Van Cleuvenbergen, S. Deckers, C. Kumara, A. Dass, H. Häkkinen, K. Clays, T. Verbiest and S. Knoppe, *Nanoscale*, 2016, **8**, 12123–12127.

96 Z. Wu, E. Lanni, W. Chen, M. E. Bier, D. Ly and R. Jin, *J. Am. Chem. Soc.*, 2009, **131**, 16672–16674.

97 H. Yao, *J. Phys. Chem. Lett.*, 2012, **3**, 1701–1706.

98 H. Yao and R. Kobayashi, *J. Colloid Interface Sci.*, 2014, **419**, 1–8.

99 H. Yao, R. Kobayashi and Y. Nonoguchi, *J. Phys. Chem. C*, 2016, **120**, 1284–1292.

100 H. Yao and T. Shiratsu, *Chem. Lett.*, 2017, **46**, 104–107.

101 Y. Levi-Kalisman, P. D. Jadzinsky, N. Kalisman, H. Tsunoyama, T. Tsukuda, D. A. Bushnell and R. D. Kornberg, *J. Am. Chem. Soc.*, 2011, **133**, 2976–2982.

102 M. Azubel and R. D. Kornberg, *Nano Lett.*, 2016, **16**, 3348–3351.

103 T. Chen, V. Fung, Q. Yao, Z. Luo, D.-e. Jiang and J. Xie, *J. Am. Chem. Soc.*, 2018, **140**, 11370–11377.

104 T. Chen, Z. Luo, Q. Yao, A. X. H. Yeo and J. Xie, *Chem. Commun.*, 2016, **52**, 9522–9525.

105 C. Gautier and T. Bürgi, *J. Am. Chem. Soc.*, 2008, **130**, 7077–7084.

106 Z. P. Guven, B. Ustbas, K. M. Harkness, H. Coskun, C. P. Joshi, T. M. D. Besong, F. Stellacci, O. M. Bakr and O. Akbulut, *Dalton Trans.*, 2016, **45**, 11297–11300.

107 V. Marjomäki, T. Lahtinen, M. Martikainen, J. Koivisto, S. Malola, K. Salorinne, M. Pettersson and H. Häkkinen, *Proc. Natl. Acad. Sci. U. S. A.*, 2014, **111**, 1277–1281.

108 E. Porret, M. Jourdan, B. Gennaro, C. Comby-Zerbino, F. Bertorelle, V. Trouillet, X. Qiu, C. Zoukimian, D. Boturyn, N. Hildebrandt, R. Antoine, J.-L. Coll and X. Le Guével, *J. Phys. Chem. C*, 2019, **123**, 26705–26717.

109 H. Yao, N. Kitaoka and A. Sasaki, *Nanoscale*, 2012, **4**, 955–963.

110 H. Yao and S. Yaomura, *Langmuir*, 2013, **29**, 6444–6451.

111 T. A. Dreier, W. S. Compel, O. A. Wong and C. J. Ackerson, *J. Phys. Chem. C*, 2016, **120**, 28288–28294.

112 M. S. Bootharaju, V. M. Burlakov, T. M. D. Besong, C. P. Joshi, L. G. AbdulHalim, D. M. Black, R. L. Whetten, A. Goriely and O. M. Bakr, *Chem. Mater.*, 2015, **27**, 4289–4297.

113 Y. Yu, J. Li, T. Chen, Y. N. Tan and J. Xie, *J. Phys. Chem. C*, 2015, **119**, 10910–10918.

114 J. Zheng and R. M. Dickson, *J. Am. Chem. Soc.*, 2002, **124**, 13982–13983.

115 J. Zheng, C. Zhang and R. M. Dickson, *Phys. Rev. Lett.*, 2004, **93**, 077402.

116 L.-Y. Chen, C.-W. Wang, Z. Yuan and H.-T. Chang, *Anal. Chem.*, 2015, **87**, 216–229.

117 T. Udayabhaskararao and T. Pradeep, *Angew. Chem., Int. Ed.*, 2010, **49**, 3925–3929.

118 O. A. Wong, C. L. Heinecke, A. R. Simone, R. L. Whetten and C. J. Ackerson, *Nanoscale*, 2012, **4**, 4099–4102.

119 T. Lahtinen, E. Hulkko, K. Sokołowska, T.-R. Tero, V. Saarnio, J. Lindgren, M. Pettersson, H. Häkkinen and L. Lehtovaara, *Nanoscale*, 2016, **8**, 18665–18674.

120 W. E. C. Moore, D. E. Hash, L. V. Holdeman and E. P. Cato, *Appl. Environ. Microbiol.*, 1980, **39**, 900–907.

121 M. C. Stark, M. A. Baikoghli, T. Lahtinen, S. Malola, L. Xing, M. Nguyen, M. Nguyen, A. Sikaroudi, V. Marjomäki, H. Häkkinen and R. H. Cheng, *Sci. Rep.*, 2017, **7**, 17048.

122 A. M. Al-Somali, K. M. Krueger, J. C. Falkner and V. L. Colvin, *Anal. Chem.*, 2004, **76**, 5903–5910.

123 R. Balasubramanian, R. Guo, A. J. Mills and R. W. Murray, *J. Am. Chem. Soc.*, 2005, **127**, 8126–8132.

124 D. M. Black, G. Robles, S. B. H. Bach and R. L. Whetten, *Ind. Eng. Chem. Res.*, 2018, **57**, 5378–5384.

125 M. R. Branham, A. D. Douglas, A. J. Mills, J. B. Tracy, P. S. White and R. W. Murray, *Langmuir*, 2006, **22**, 11376–11383.

126 A. Dass, R. Guo, J. B. Tracy, R. Balasubramanian, A. D. Douglas and R. W. Murray, *Langmuir*, 2008, **24**, 310–315.

127 M. Galchenko, R. Schuster, A. Black, M. Riedner and C. Klinke, *Nanoscale*, 2019, **11**, 1988–1994.

128 A. Ghosh and T. Pradeep, *Eur. J. Inorg. Chem.*, 2014, **2014**, 5271–5275.

129 S. Hossain, W. Kurashige, S. Wakayama, B. Kumar, L. V. Nair, Y. Niihori and Y. Negishi, *J. Phys. Chem. C*, 2016, **120**, 25861–25869.

130 Y. Ishida, A. Morita, T. Tokunaga and T. Yonezawa, *Langmuir*, 2018, **34**, 4024–4030.

131 S. Knoppe, J. Boudon, I. Dolamic, A. Dass and T. Bürgi, *Anal. Chem.*, 2011, **83**, 5056–5061.

132 D. Lee, R. L. Donkers, J. M. DeSimone and R. W. Murray, *J. Am. Chem. Soc.*, 2003, **125**, 1182–1183.

133 S. Matsuo, S. Yamazoe, J.-Q. Goh, J. Akola and T. Tsukuda, *Phys. Chem. Chem. Phys.*, 2016, **18**, 4822–4827.

134 L. D. Menard, S.-P. Gao, H. Xu, R. D. Twesten, A. S. Harper, Y. Song, G. Wang, A. D. Douglas, J. C. Yang, A. I. Frenkel, R. G. Nuzzo and R. W. Murray, *J. Phys. Chem. B*, 2006, **110**, 12874–12883.

135 Y. Negishi, U. Kamimura, M. Ide and M. Hirayama, *Nanoscale*, 2012, **4**, 4263–4268.

136 H. Qian, E. Barry, Y. Zhu and R. Jin, *Acta Phys. -Chim. Sin.*, 2011, **27**, 513–519.

137 H. Qian, D.-e. Jiang, G. Li, C. Gayathri, A. Das, R. R. Gil and R. Jin, *J. Am. Chem. Soc.*, 2012, **134**, 16159–16162.

138 H. Qian, M. Zhu, U. N. Andersen and R. Jin, *J. Phys. Chem. A*, 2009, **113**, 4281–4284.

139 H. Qian, Y. Zhu and R. Jin, *ACS Nano*, 2009, **3**, 3795–3803.

140 K. G. Stamplecoskie, G. Yousefalizadeh, L. Gozdzialski and H. Ramsay, *J. Phys. Chem. C*, 2018, **122**, 13738–13744.

141 Z. Tang, D. A. Robinson, N. Bokossa, B. Xu, S. Wang and G. Wang, *J. Am. Chem. Soc.*, 2011, **133**, 16037–16044.

142 H. Tsunoyama, P. Nickut, Y. Negishi, K. Al-Shamery, Y. Matsumoto and T. Tsukuda, *J. Phys. Chem. C*, 2007, **111**, 4153–4158.

143 X. Wei, X. Kang, S. Wang and M. Zhu, *Dalton Trans.*, 2018, **47**, 13766–13770.

144 J. Xiang, P. Li, Y. Song, X. Liu, H. Chong, S. Jin, Y. Pei, X. Yuan and M. Zhu, *Nanoscale*, 2015, **7**, 18278–18283.

145 M. Zhu, H. Qian and R. Jin, *J. Am. Chem. Soc.*, 2009, **131**, 7220–7221.

146 V. L. Jimenez, M. C. Leopold, C. Mazzitelli, J. W. Jorgenson and R. W. Murray, *Anal. Chem.*, 2003, **75**, 199–206.

147 Y. Song, M. L. Heien, V. Jimenez, R. M. Wightman and R. W. Murray, *Anal. Chem.*, 2004, **76**, 4911–4919.

148 Y. Song, V. Jimenez, C. McKinney, R. Donkers and R. W. Murray, *Anal. Chem.*, 2003, **75**, 5088–5096.

149 R. L. Wolfe and R. W. Murray, *Anal. Chem.*, 2006, **78**, 1167–1173.

150 Y. Negishi, C. Sakamoto, T. Ohyama and T. Tsukuda, *J. Phys. Chem. Lett.*, 2012, **3**, 1624–1628.

151 H. Qian and R. Jin, *Nano Lett.*, 2009, **9**, 4083–4087.

152 A. Tlahuice-Flores, U. Santiago, D. Bahena, E. Vinogradova, C. V. Conroy, T. Ahuja, S. B. H. Bach, A. Ponce, G. Wang, M. José-Yacamán and R. L. Whetten, *J. Phys. Chem. A*, 2013, **117**, 10470–10476.

153 Y. Chen, C. Zeng, C. Liu, K. Kirschbaum, C. Gayathri, R. R. Gil, N. L. Rosi and R. Jin, *J. Am. Chem. Soc.*, 2015, **137**, 10076–10079.

154 Y. Negishi, T. Nakazaki, S. Malola, S. Takano, Y. Niihori, W. Kurashige, S. Yamazoe, T. Tsukuda and H. Häkkinen, *J. Am. Chem. Soc.*, 2015, **137**, 1206–1212.

155 M. Zhou, C. Zeng, Y. Song, J. W. Padelford, G. Wang, M. Y. Sfeir, T. Higaki and R. Jin, *Angew. Chem., Int. Ed.*, 2017, **56**, 16257–16261.

156 T. Higaki, M. Zhou, K. J. Lambright, K. Kirschbaum, M. Y. Sfeir and R. Jin, *J. Am. Chem. Soc.*, 2018, **140**, 5691–5695.

157 N. A. Sakthivel, S. Theivendran, V. Ganeshraj, A. G. Oliver and A. Dass, *J. Am. Chem. Soc.*, 2017, **139**, 15450–15459.

158 N. A. Sakthivel, M. Stener, L. Sementa, A. Fortunelli, G. Ramakrishna and A. Dass, *J. Phys. Chem. Lett.*, 2018, **9**, 1295–1300.

159 S. Knoppe and P. Vogt, *Anal. Chem.*, 2019, **91**, 1603–1609.

160 D. M. Black, S. B. H. Bach and R. L. Whetten, *Anal. Chem.*, 2016, **88**, 5631–5636.

161 D. M. Black, N. Bhattarai, S. B. H. Bach and R. L. Whetten, *J. Phys. Chem. Lett.*, 2016, **7**, 3199–3205.

162 Y. Negishi, W. Kurashige, Y. Niihori, T. Iwasa and K. Nobusada, *Phys. Chem. Chem. Phys.*, 2010, **12**, 6219–6225.

163 Y. Negishi, T. Iwai and M. Ide, *Chem. Commun.*, 2010, **46**, 4713–4715.

164 C. Kumara, C. M. Aikens and A. Dass, *J. Phys. Chem. Lett.*, 2014, **5**, 461–466.

165 S. Tian, L. Liao, J. Yuan, C. Yao, J. Chen, J. Yang and Z. Wu, *Chem. Commun.*, 2016, **52**, 9873–9876.

166 Z. Wu and R. Jin, *Nano Lett.*, 2010, **10**, 2568–2573.

167 Y. Negishi, H. Tsunoyama, Y. Yanagimoto and T. Tsukuda, *Chem. Lett.*, 2005, **34**, 1638–1639.

168 A. Dass, A. Stevenson, G. R. Dubay, J. B. Tracy and R. W. Murray, *J. Am. Chem. Soc.*, 2008, **130**, 5940–5946.

169 V. R. Jupally, R. Kota, E. V. Dornshuld, D. L. Mattern, G. S. Tschumper, D.-e. Jiang and A. Dass, *J. Am. Chem. Soc.*, 2011, **133**, 20258–20266.

170 J. B. Tracy, M. C. Crowe, J. F. Parker, O. Hampe, C. A. Fields-Zinna, A. Dass and R. W. Murray, *J. Am. Chem. Soc.*, 2007, **129**, 16209–16215.

171 Y. Niihori, M. Matsuzaki, T. Pradeep and Y. Negishi, *J. Am. Chem. Soc.*, 2013, **135**, 4946–4949.

172 Y. Niihori, M. Matsuzaki, C. Uchida and Y. Negishi, *Nanoscale*, 2014, **6**, 7889–7896.

173 Y. Niihori, Y. Kikuchi, A. Kato, M. Matsuzaki and Y. Negishi, *ACS Nano*, 2015, **9**, 9347–9356.

174 M. S. Bootharaju, C. P. Joshi, M. R. Parida, O. F. Mohammed and O. M. Bakr, *Angew. Chem., Int. Ed.*, 2016, **55**, 922–926.

175 J. C. Gonzalez and A. Muñoz-Castro, *J. Phys. Chem. C*, 2016, **120**, 27019–27026.

176 M. Ganguly, C. Mondal, J. Pal, A. Pal, Y. Negishi and T. Pal, *Dalton Trans.*, 2014, **43**, 11557–11565.

177 E. B. Guidez, V. Mäkinen, H. Häkkinen and C. M. Aikens, *J. Phys. Chem. C*, 2012, **116**, 20617–20624.

178 S. Hossain, Y. Imai, Y. Motohashi, Z. Chen, D. Suzuki, T. Suzuki, Y. Kataoka, M. Hirata, T. Ono, W. Kurashige, T. Kawawaki, T. Yamamoto and Y. Negishi, *Mater. Horiz.*, 2020, **7**, 796–803.

179 S. Hossain, Y. Imai and Y. Negishi, *AIP Conf. Proc.*, 2019, **2186**, 030018.

180 S. Hossain, Y. Imai, D. Suzuki, W. Choi, Z. Chen, T. Suzuki, M. Yoshioka, T. Kawawaki, D. Lee and Y. Negishi, *Nanoscale*, 2019, **11**, 22089–22098.

181 S. Hossain, T. Ono, M. Yoshioka, G. Hu, M. Hosoi, Z. Chen, L. V. Nair, Y. Niihori, W. Kurashige, D.-e. Jiang and Y. Negishi, *J. Phys. Chem. Lett.*, 2018, **9**, 2590–2594.

182 J. Jana, T. Aditya, Y. Negishi and T. Pal, *ACS Omega*, 2017, **2**, 8086–8098.

183 D.-e. Jiang and S. Dai, *Inorg. Chem.*, 2009, **48**, 2720–2722.

184 R. Jin and K. Nobusada, *Nano Res.*, 2014, **7**, 285–300.

185 W. Kurashige, R. Hayashi, K. Wakamatsu, Y. Kataoka, S. Hossain, A. Iwase, A. Kudo, S. Yamazoe and Y. Negishi, *ACS Appl. Energy Mater.*, 2019, **2**, 4175–4187.

186 W. Kurashige, K. Munakata, K. Nobusada and Y. Negishi, *Chem. Commun.*, 2013, **49**, 5447–5449.

187 W. Kurashige and Y. Negishi, *J. Cluster Sci.*, 2012, **23**, 365–374.

188 W. Kurashige, Y. Niihori, S. Sharma and Y. Negishi, *J. Phys. Chem. Lett.*, 2014, **5**, 4134–4142.

189 W. Kurashige, Y. Niihori, S. Sharma and Y. Negishi, *Coord. Chem. Rev.*, 2016, **320–321**, 238–250.

190 B. Molina and A. Tlahuice-Flores, *Phys. Chem. Chem. Phys.*, 2016, **18**, 1397–1403.

191 L. V. Nair, S. Hossain, S. Takagi, Y. Imai, G. Hu, S. Wakayama, B. Kumar, W. Kurashige, D.-e. Jiang and Y. Negishi, *Nanoscale*, 2018, **10**, 18969–18979.

192 Y. Negishi, W. Kurashige, Y. Kobayashi, S. Yamazoe, N. Kojima, M. Seto and T. Tsukuda, *J. Phys. Chem. Lett.*, 2013, **4**, 3579–3583.

193 Y. Negishi, W. Kurashige, Y. Niihori and K. Nobusada, *Phys. Chem. Chem. Phys.*, 2013, **15**, 18736–18751.

194 Y. Negishi, K. Munakata, W. Ohgake and K. Nobusada, *J. Phys. Chem. Lett.*, 2012, **3**, 2209–2214.

195 Y. Niihori, M. Eguro, A. Kato, S. Sharma, B. Kumar, W. Kurashige, K. Nobusada and Y. Negishi, *J. Phys. Chem. C*, 2016, **120**, 14301–14309.

196 Y. Niihori, S. Hossain, B. Kumar, L. V. Nair, W. Kurashige and Y. Negishi, *APL Mater.*, 2017, **5**, 053201.

197 Y. Niihori, S. Hossain, S. Sharma, B. Kumar, W. Kurashige and Y. Negishi, *Chem. Rec.*, 2017, **17**, 473–484.

198 Y. Niihori, W. Kurashige, M. Matsuzaki and Y. Negishi, *Nanoscale*, 2013, **5**, 508–512.

199 Y. Niihori, K. Yoshida, S. Hossain, W. Kurashige and Y. Negishi, *Bull. Chem. Soc. Jpn.*, 2019, **92**, 664–695.

200 A. Puls, P. Jerabek, W. Kurashige, M. Förster, M. Molon, T. Bollermann, M. Winter, C. Gemel, Y. Negishi, G. Frenking and R. A. Fischer, *Angew. Chem., Int. Ed.*, 2014, **53**, 4327–4331.

201 S. Sharma, W. Kurashige, K. Nobusada and Y. Negishi, *Nanoscale*, 2015, **7**, 10606–10612.

202 S. Sharma, S. Yamazoe, T. Ono, W. Kurashige, Y. Niihori, K. Nobusada, T. Tsukuda and Y. Negishi, *Dalton Trans.*, 2016, **45**, 18064–18068.

203 M. A. Tofanelli, T. W. Ni, B. D. Phillips and C. J. Ackerson, *Inorg. Chem.*, 2016, **55**, 999–1001.

204 S. Xie, H. Tsunoyama, W. Kurashige, Y. Negishi and T. Tsukuda, *ACS Catal.*, 2012, **2**, 1519–1523.

205 S. Yamazoe, W. Kurashige, K. Nobusada, Y. Negishi and T. Tsukuda, *J. Phys. Chem. C*, 2014, **118**, 25284–25290.

206 H. Yang, Y. Wang, H. Huang, L. Gell, L. Lehtovaara, S. Malola, H. Häkkinen and N. Zheng, *Nat. Commun.*, 2013, **4**, 2422.

207 Q. Yao, Y. Feng, V. Fung, Y. Yu, D.-e. Jiang, J. Yang and J. Xie, *Nat. Commun.*, 2017, **8**, 1555.

208 T. Yokoyama, N. Hirata, H. Tsunoyama, Y. Negishi and A. Nakajima, *AIP Adv.*, 2018, **8**, 065002.

209 B. Zhang, S. Kaziz, H. Li, D. Wodka, S. Malola, O. Safonova, M. Nachtegaal, C. Mazet, I. Dolamic, J. Llorca, E. Kalenius, L. M. L. Daku, H. Häkkinen, T. Bürgi and N. Barrabés, *Nanoscale*, 2015, **7**, 17012–17019.

210 S. Wang, Y. Song, S. Jin, X. Liu, J. Zhang, Y. Pei, X. Meng, M. Chen, P. Li and M. Zhu, *J. Am. Chem. Soc.*, 2015, **137**, 4018–4021.

211 Y. Niihori, D. Shima, K. Yoshida, K. Hamada, L. V. Nair, S. Hossain, W. Kurashige and Y. Negishi, *Nanoscale*, 2018, **10**, 1641–1649.

212 Y. Niihori, Y. Koyama, S. Watanabe, S. Hashimoto, S. Hossain, L. V. Nair, B. Kumar, W. Kurashige and Y. Negishi, *J. Phys. Chem. Lett.*, 2018, **9**, 4930–4934.

213 Y. Niihori, S. Hashimoto, Y. Koyama, S. Hossain, W. Kurashige and Y. Negishi, *J. Phys. Chem. C*, 2019, **123**, 13324–13329.

214 C. Kumara and A. Dass, *Nanoscale*, 2012, **4**, 4084–4086.

215 Y. Niihori, Y. Kikuchi, D. Shima, C. Uchida, S. Sharma, S. Hossain, W. Kurashige and Y. Negishi, *Ind. Eng. Chem. Res.*, 2017, **56**, 1029–1035.

216 M. M. F. Choi, A. D. Douglas and R. W. Murray, *Anal. Chem.*, 2006, **78**, 2779–2785.

217 Y. Zhang, S. Shuang, C. Dong, C. K. Lo, M. C. Paau and M. M. F. Choi, *Anal. Chem.*, 2009, **81**, 1676–1685.

218 M. C. Paau, Q. Hu, Y. Zhang and M. M. F. Choi, *Anal. Methods*, 2015, **7**, 2452–2457.

219 L. Zhang, Q. Hu, Z. Li, Y. Zhang, D. Lu, S. Shuang, M. M. F. Choi and C. Dong, *Anal. Methods*, 2017, **9**, 4539–4546.

220 D. M. Black, M. M. Alvarez, F. Yan, W. P. Griffith, G. Plascencia-Villa, S. B. H. Bach and R. L. Whetten, *J. Phys. Chem. C*, 2017, **121**, 10851–10857.

221 D. M. Black, M. M. Hoque, G. Plascencia-Villa and R. L. Whetten, *Nanomaterials*, 2019, **9**, 1303.

222 D. M. Black, G. Robles, P. Lopez, S. B. H. Bach, M. Alvarez and R. L. Whetten, *Anal. Chem.*, 2018, **90**, 2010–2017.

223 P. Lopez, H. H. Lara, S. M. Mullins, D. M. Black, H. M. Ramsower, M. M. Alvarez, T. L. Williams, X. Lopez-Lozano, H.-C. Weissker, A. P. García, I. L. Garzón, B. Demeler, J. L. Lopez-Ribot, M. J. Yacamán and R. L. Whetten, *ACS Appl. Nano Mater.*, 2018, **1**, 1595–1602.

224 B. Buszewski and S. Noga, *Anal. Bioanal. Chem.*, 2012, **402**, 231–247.

225 H. Ramsay, D. Simon, E. Steele, A. Hebert, R. D. Oleschuk and K. G. Stamplecoskie, *RSC Adv.*, 2018, **8**, 42080–42086.

226 J. P. Wilcoxon, J. E. Martin and P. Provencio, *Langmuir*, 2000, **16**, 9912–9920.

227 H. Murayama, T. Narushima, Y. Negishi and T. Tsukuda, *J. Phys. Chem. B*, 2004, **108**, 3496–3503.

228 J. P. Wilcoxon, J. E. Martin and P. Provencio, *J. Chem. Phys.*, 2001, **115**, 998–1008.

229 J. P. Wilcoxon and P. Provencio, *J. Phys. Chem. B*, 2003, **107**, 12949–12957.

230 H. Tsunoyama, Y. Negishi and T. Tsukuda, *J. Am. Chem. Soc.*, 2006, **128**, 6036–6037.

231 R. Tsunoyama, H. Tsunoyama, P. Pannopard, J. Limtrakul and T. Tsukuda, *J. Phys. Chem. C*, 2010, **114**, 16004–16009.

232 H. Qian and R. Jin, *Chem. Commun.*, 2011, **47**, 11462–11464.

233 H. Qian, Y. Zhu and R. Jin, *J. Am. Chem. Soc.*, 2010, **132**, 4583–4585.

234 Y. Negishi, R. Arai, Y. Niihori and T. Tsukuda, *Chem. Commun.*, 2011, **47**, 5693–5695.

235 Z. Wu, M. A. MacDonald, J. Chen, P. Zhang and R. Jin, *J. Am. Chem. Soc.*, 2011, **133**, 9670–9673.

236 X. Zhu, S. Jin, S. Wang, X. Meng, C. Zhu, M. Zhu and R. Jin, *Chem. – Asian J.*, 2013, **8**, 2739–2745.

237 S.-i. Tanaka, J. Miyazaki, D. K. Tiwari, T. Jin and Y. Inouye, *Angew. Chem., Int. Ed.*, 2011, **50**, 431–435.

238 S.-i. Tanaka, K. Aoki, A. Muratsugu, H. Ishitobi, T. Jin and Y. Inouye, *Opt. Mater. Express*, 2013, **3**, 157–165.

239 C. E. Dalgliesh, *J. Chem. Soc.*, 1952, 3940–3942.

240 P. D. Jadzinsky, G. Calero, C. J. Ackerson, D. A. Bushnell and R. D. Kornberg, *Science*, 2007, **318**, 430–433.

241 C. Zeng, Y. Chen, K. Kirschbaum, K. Appavoo, M. Y. Sfeir and R. Jin, *Sci. Adv.*, 2015, **1**, e1500045.

242 C. Zeng, T. Li, A. Das, N. L. Rosi and R. Jin, *J. Am. Chem. Soc.*, 2013, **135**, 10011–10013.

243 C. Zeng, C. Liu, Y. Chen, N. L. Rosi and R. Jin, *J. Am. Chem. Soc.*, 2014, **136**, 11922–11925.

244 I. Dolamic, S. Knoppe, A. Dass and T. Bürgi, *Nat. Commun.*, 2012, **3**, 798.

245 S. Knoppe, I. Dolamic and T. Bürgi, *J. Am. Chem. Soc.*, 2012, **134**, 13114–13120.

246 B. Varnholt, I. Dolamic, S. Knoppe and T. Bürgi, *Nanoscale*, 2013, **5**, 9568–9571.

247 S. Knoppe, R. Azoulay, A. Dass and T. Bürgi, *J. Am. Chem. Soc.*, 2012, **134**, 20302–20305.

248 S. Knoppe, S. Michalet and T. Bürgi, *J. Phys. Chem. C*, 2013, **117**, 15354–15361.

249 K. Soai, T. Shibata, H. Morioka and K. Choji, *Nature*, 1995, **378**, 767–768.

250 Tokyo University of Science, *Jpn. Pat*, P2018-135292A, 2018.

251 L. Beqa, D. Deschamps, S. Perrio, A.-C. Gaumont, S. Knoppe and T. Bürgi, *J. Phys. Chem. C*, 2013, **117**, 21619–21625.

252 I. Dolamic, B. Varnholt and T. Bürgi, *Nat. Commun.*, 2015, **6**, 7117.

253 S. Jin, F. Xu, W. Du, X. Kang, S. Chen, J. Zhang, X. Li, D. Hu, S. Wang and M. Zhu, *Inorg. Chem.*, 2018, **57**, 5114–5119.

254 R. Kazan, B. Zhang and T. Bürgi, *Dalton Trans.*, 2017, **46**, 7708–7713.

255 N. Barrabés, B. Zhang and T. Bürgi, *J. Am. Chem. Soc.*, 2014, **136**, 14361–14364.

256 X. Liu, J. Yuan, J. Chen, J. Yang and Z. Wu, *Part. Part. Syst. Charact.*, 2019, **36**, 1900003.

257 A. Sels, N. Barrabés, S. Knoppe and T. Bürgi, *Nanoscale*, 2016, **8**, 11130–11135.

258 A. Sels, G. Salassa, S. Pollitt, C. Guglieri, G. Rupprechter, N. Barrabés and T. Bürgi, *J. Phys. Chem. C*, 2017, **121**, 10919–10926.

259 S. Knoppe, I. Dolamic, A. Dass and T. Bürgi, *Angew. Chem., Int. Ed.*, 2012, **51**, 7589–7591.

260 B. Varnholt, R. Letrun, J. J. Bergkamp, Y. Fu, O. Yushchenko, S. Decurtins, E. Vauthey, S.-X. Liu and T. Bürgi, *Phys. Chem. Chem. Phys.*, 2015, **17**, 14788–14795.

261 B. Zhang and T. Bürgi, *J. Phys. Chem. C*, 2016, **120**, 4660–4666.

262 A. Ushiyama, S. Hiroto, J. Yuasa, T. Kawai and H. Shinokubo, *Org. Chem. Front.*, 2017, **4**, 664–667.

263 N. Yan, N. Xia, L. Liao, M. Zhu, F. Jin, R. Jin and Z. Wu, *Sci. Adv.*, 2018, **4**, eaat7259.

264 A. Ghosh, J. Hassinen, P. Pulkkinen, H. Tenhu, R. H. A. Ras and T. Pradeep, *Anal. Chem.*, 2014, **86**, 12185–12190.

265 C. Yao, J. Chen, M.-B. Li, L. Liu, J. Yang and Z. Wu, *Nano Lett.*, 2015, **15**, 1281–1287.

266 S. Tian, Y.-Z. Li, M.-B. Li, J. Yuan, J. Yang, Z. Wu and R. Jin, *Nat. Commun.*, 2015, **6**, 8667.

267 S. Tian, C. Yao, L. Liao, N. Xia and Z. Wu, *Chem. Commun.*, 2015, **51**, 11773–11776.

268 L. Liao, C. Yao, C. Wang, S. Tian, J. Chen, M.-B. Li, N. Xia, N. Yan and Z. Wu, *Anal. Chem.*, 2016, **88**, 11297–11301.

269 Q. Yao, V. Fung, C. Sun, S. Huang, T. Chen, D.-e. Jiang, J. Y. Lee and J. Xie, *Nat. Commun.*, 2018, **9**, 1979.

270 D. R. Stoll and P. W. Carr, *J. Am. Chem. Soc.*, 2005, **127**, 5034–5035.